AWARD NUMBER: W81XWH-20-1-0241

TITLE: *RNA-Based Approach to Decrease TDP-43 Pathology and Neurotoxicity in ALS*

PRINCIPAL INVESTIGATOR: Yuna M. Ayala

CONTRACTING ORGANIZATION: Saint Louis University, St. Louis, MO

REPORT DATE: July 2021

TYPE OF REPORT: Annual

PREPARED FOR: U.S. Army Medical Research and Development Command
Fort Detrick, Maryland 21702-5012

DISTRIBUTION STATEMENT: Approved for Public Release;
Distribution Unlimited

The views, opinions and/or findings contained in this report are those of the author(s) and should not be construed as an official Department of the Army position, policy or decision unless so designated by other documentation.

REPORT DOCUMENTATION PAGE

Form Approved
OMB No. 0704-0188

Public reporting burden for this collection of information is estimated to average 1 hour per response, including the time for reviewing instructions, searching existing data sources, gathering and maintaining the data needed, and completing and reviewing this collection of information. Send comments regarding this burden estimate or any other aspect of this collection of information, including suggestions for reducing this burden to Department of Defense, Washington Headquarters Services, Directorate for Information Operations and Reports (0704-0188), 1215 Jefferson Davis Highway, Suite 1204, Arlington, VA 22202-4302. Respondents should be aware that notwithstanding any other provision of law, no person shall be subject to any penalty for failing to comply with a collection of information if it does not display a currently valid OMB control number. **PLEASE DO NOT RETURN YOUR FORM TO THE ABOVE ADDRESS.**

1. REPORT DATE	2. REPORT TYPE	3. DATES COVERED
July 2021	Annual	01Jul2020-30Jun2021

4. TITLE AND SUBTITLE

RNA-Based Approach to Decrease TDP-43 Pathology and Neurotoxicity in ALS

5a. CONTRACT NUMBER

5b. GRANT NUMBER
W81XWH-20-1-0241

5c. PROGRAM ELEMENT NUMBER

6. AUTHOR(S)
Yuna M. Ayala and Timothy M. Miller

E-Mail: yuna.ayala@health.slu.edu, miller.t@wustl.edu

5d. PROJECT NUMBER

5e. TASK NUMBER

5f. WORK UNIT NUMBER

7. PERFORMING ORGANIZATION NAME(S) AND ADDRESS(ES)

AND ADDRESS(ES)

Saint Louis University
Department of Biochemistry
and Molecular Biology
1100 S. Grand Blvd

Washington University, St. Louis
Department of Neurology
660 S. Euclid
St. Louis, MO 63110

8. PERFORMING ORGANIZATION REPORT NUMBER

9. SPONSORING / MONITORING AGENCY NAME(S) AND ADDRESS(ES)

U.S. Army Medical Research and Development Command
Fort Detrick, Maryland 21702-5012

10. SPONSOR/MONITOR'S ACRONYM(S)

11. SPONSOR/MONITOR'S REPORT NUMBER(S)

12. DISTRIBUTION / AVAILABILITY STATEMENT

Approved for Public Release; Distribution Unlimited

13. SUPPLEMENTARY NOTES

14. ABSTRACT

The aggregation of the TAR DNA binding protein (TDP-43) is the hallmark feature of ALS. TDP-43 aggregates found in the brain and spinal cord of almost all ALS patients are associated with toxicity and loss of cell viability. Our project will leverage our position as experts in TDP-43 biology and use the tools we have developed to analyze TDP-43 aggregation and inhibit this pathogenic process. We recently found that RNA molecules are potent inhibitors of TDP-43 aggregation, which leads us to ask: *Can specific RNA molecules be used to prevent TDP-43 aggregation and decrease neurotoxicity?* This question will be tested using our established methods using purified TDP-43, human cellular models and mouse models of ALS. Dr. Timothy Miller, the co-Principal Investigator in this proposal, and his team are experts in using RNA to reduce neurodegeneration in various models and in first-in-kind patient clinical trials. Together, our team will screen and identify new molecules to effectively reduce TDP-43 aggregation and its associated pathology.

15. SUBJECT TERMS
Amyotrophic lateral sclerosis (ALS), neurodegeneration, TDP-43 (TAR DNA binding protein), RNA, protein aggregation, RNA binding proteins

16. SECURITY CLASSIFICATION OF:			17. LIMITATION OF ABSTRACT	18. NUMBER OF PAGES	19a. NAME OF RESPONSIBLE PERSON
a. REPORT	b. ABSTRACT	c. THIS PAGE			USAMRMC
Unclassified	Unclassified	Unclassified	Unclassified	69	19b. TELEPHONE NUMBER *(include area code)*

TABLE OF CONTENTS

Page

1. **Introduction……2**
2. **Keywords ……2**
3. **Accomplishments…… 3-8**
4. **Impact…… 10**
5. **Changes/Problems…… 10**
6. **Products……..…… 11**
7. **Participants & Other Collaborating Organizations……11**
8. **Special Reporting Requirements……11**
9. **Appendices……11**

1. **Introduction.**

This proposal is responsive to ongoing efforts to treat and cure Amyotrophic Lateral Sclerosis (ALS), also known as Lou Gehrig's disease. ALS is a devastating neurodegenerative disorder for which there is no cure or efficient detection tools. We seek to accelerate the development of new therapeutic molecules to reduce neurodegeneration and toxicity in ALS.

ALS is a late onset neurodegenerative and fatal disease that affects women and men worldwide and leads to muscle atrophy in patients. In a portion of these cases, ALS is linked to cognitive impairment associated with frontotemporal lobar degeneration or frontotemporal dementia. On average, ALS strikes patients in their 60s and some clinicians have reported an increase in the number of 20-30 year old patients diagnosed with ALS. *According to existing evidence, military men and women are twice as likely to be affected by ALS than non-military individuals,* regardless of whether the individual served in combat or not. Among the possible explanations for this increased risk are elevated stress and traumatic brain injury during training or combat. ALS causes the death of individuals, often from respiratory failure, two to five years post-diagnosis. Therefore, it is imperative to develop strategies to decrease the factors contributing to the development of ALS.

TAR DNA-binding protein (TDP-43) aggregation and loss of function is the hallmark of almost all familial and sporadic ALS cases. TDP-43 inclusions accumulate in neurons and glial cells in the brain and spinal cord. These deposits coincide with a dramatic reduction of normal nuclear TDP-43 detection, implying a loss of function upon aggregation. This is viewed as a major factor impeding neuronal function as TDP-43 is known to be essential for development and survival. Whether disease results from aggregate toxicity, from sequestration of functional TDP-43 into aggregates, or from a combination of both mechanisms is yet unclear. Either way, reducing the accumulation of TDP-43 aggregates is a major goal to decrease neurodegeneration. We found that TDP-43 binding to RNA strongly inhibits its aggregation depending on nucleotide sequence composition. These findings strongly suggest that RNA acts as a chaperone maintaining TDP-43 solubility and leads us to ask: *Can specific RNA molecules be used to prevent TDP-43 aggregation and decrease neurotoxicity?* This question is being tested using our established methods using purified TDP-43, human cellular models and mouse models of ALS. Dr. Timothy Miller, the co-Principal Investigator in this proposal, and his team are experts in using RNA to reduce neurodegeneration in various models and in first-in-kind patient clinical trials. Further, Dr. Miller is the director of the Washington University ALS Center. As a physician, Dr. Miller is dedicated to providing quality care and state-of-the-art treatment to ALS patients. Together, our team will screen and identify new molecules to effectively reduce TDP-43 aggregation and its associated pathology.

2. **Keywords**

Amyotrophic lateral sclerosis (ALS), neurodegeneration, TDP-43 (TAR DNA binding protein), RNA, protein aggregation, RNA binding proteins

3. **Accomplishments**

What were the major goals of the project?

Based on our earlier observations, we hypothesize that specific RNA molecules may be used to decrease TDP-43 aggregation, which will reduce toxicity and restore protein function. We sought to design specific RNA molecules that significantly prevent TDP-43 aggregation without causing loss of protein function or cell toxicity and to test their efficacy using various models of TDP-43 pathology. Our project is divided into three specific aims as follows:

Aim 1. Establish RNA-based methods to block TDP-43 aggregation. Our goal is to identify specific RNA molecules that efficiently inhibit TDP-43 aggregation, increase solubility and restore protein function. These experiments will test purified TDP-43 cultured human cell-based models.

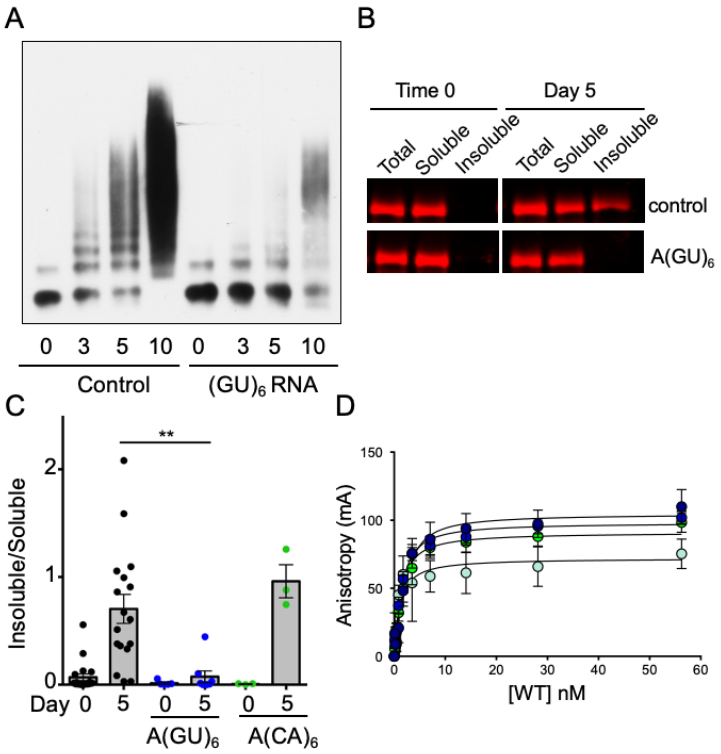
Aim 2. Determine whether RNA inhibits intracellular TDP-43 aggregate seeding and propagation. For this aim we are testing the ability of RNA to inhibit intracellular TDP-43 aggregate seeding by pre-formed fibrils. This will be performed using our established reporter cell line and seeding protocols to quantify aggregate spread.

Aim 3. Use RNA to decrease TDP-43 pathology and neurotoxicity in a mouse model of ALS. We are testing the potential use of RNA-based protocols in reducing TDP-43 pathology in vivo using a previously generated mouse model that accumulates TDP-43 pathology and develops strong neurotoxicity. For these studies we are investigating whether RNA decreases TDP-43 deposition and neurodegeneration.

What was accomplished under these goals?

Aim 1. Establish RNA-based methods to block TDP-43 aggregation:

Aim 1a: Identify RNA oligonucleotides that inhibit aggregation of purified



E

Name	RNA sequence (5'-3')	$K_{d,app}$ (nM)
$A(GU)_6$	AGUGUGUGUGUGU	0.8 ± 0.1
AUG11	GUGUGAUGAAU	24 ± 4
AUG12	GUGUGAAUGAAU	30 ± 5
CLIP34	GAGAGAGCGCGUGCAGAGACUUGGUGGUGCAUAA	40 ± 5
$A(CA)_6$	ACACACACACACA	n.s.

Figure 1. GU-rich RNA inhibits the aggregation of purified TDP-43. A) Semi-denaturing detergent agarose gel electrophoresis/immunoblotting to detect aggregation of recombinant TDP-43 as a function of time. Addition of RNA composed of GU-repeats strongly inhibits accumulation of aggregates, compared to control conditions. **B)** Immunoblotting upon extraction of soluble and insoluble fractions of purified TDP-43 at time 0 and after aggregation (Day 5) in the presence of $A(GU)_6$ RNA and control. **C)** Quantification of normalized insoluble TDP-43 from (B) after treatment with $A(GU)_6$ and control $A(CA)_6$ RNA. Means and SD of at least 3 independent replicates analyzed by one-way ANOVA ($F(5,31)=11.64$, P=<0.0001). Dunett's multiple comparisons test was used to compare treatment groups to control. **P≤0.01. **D)** Fluorescence anisotropy of different FITC-labeled $A(GU)_6$ concentrations titrated with increasing TDP-43 WT and mutants (0-65 nM). Each point is the average of >3 replicates and 3 independent experiments (SEM). Solid lines represent the best global fit to calculate the apparent dissociation constant, $K_{d,app}$. **E)** Apparent dissociation constants measured in (D) for TDP-43 binding to GU-rich RNA and the control sequence $A(CA)_6$.

TDP-43. Our preliminary studies suggest that the ability of RNA molecules to inhibit TDP-43 aggregation depends on specific binding (1). We compared the ability of RNA to decrease TDP-43 aggregation using our purified protein system and cell-based models. Our results show that guanine and uridine-rich RNA oligonucleotides are most efficient at preventing TDP-43 aggregation. We examined the aggregation of purified TDP-43 using two different assays consisting of separating soluble protein from aggregate complexes (**Fig 1**). Semi-denaturing detergent agarose gel electrophoresis (SDD-AGE) was optimized in our lab to study TDP-43 aggregate intermediates. Using this technique, we observed a dramatic decrease of TDP-43 aggregation upon addition of $(GU)_6$ (1)(**Fig 1A**). These results were supported by the quantitative comparison of soluble to insoluble TDP-43 fractions taken at time 0 and five days after triggering aggregation (**Fig 1B,C**). Here, addition of $A(GU)_6$ RNA maintained TDP-43 in the soluble fraction, inhibiting accumulation of the aggregates, relative to control conditions in the absence of RNA. As control, we used an RNA oligonucleotide of similar length, $A(CA)_6$, which previously showed no significant binding activity for TDP-43 (2). Addition of $A(CA)_6$ did not significantly alter the ratio of insoluble/soluble TDP-43, compared to control. These initial observations strongly suggest that the ability of RNA to maintain TDP-43 solubility directly correlates with specific binding. We predicted that RNA molecules with the highest binding affinity will be the strongest inhibitors of aggregation. We screened a group of 20 RNA oligonucleotides with different binding affinity for TDP-43, as measured by fluorescence anisotropy (**Fig 1D,E**). We then tested GU-rich RNA oligonucleotides with affinities in the nanomolar range using these assays and observed similar effect on decreasing TDP-43 aggregation as with $A(GU)_6$ RNA.

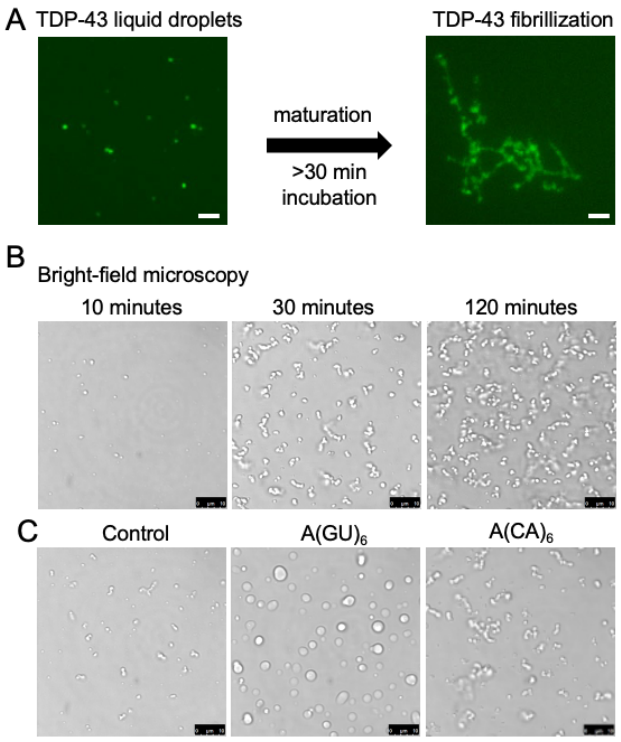


Figure 2. GU-rich RNA oligonucleotides increase the liquid properties of TDP-43 biocondensates and prevent droplet maturation. A) Representative microscope images of fluorescently labeled purified TDP-43 (0.5 μM) liquid-liquid phase separation. Incubation of samples for 30 minutes or longer resulted in fibril-like structures. Scale bars, 2 μm. **B)** Liquid droplets formed by purified TDP-43 observed by brightfield microscopy at different time points show the accumulation of 'sticky' clusters without droplet coalescence. **C)** TDP-43 droplets without RNA control or in the presence of different RNA oligonucleotide sequences (8 μM). Representative images for 3 independent experiments at 150 mM NaCl with 2 different protein preparations. Scale bars for B and C, 10 μm.

Next, we tested whether RNA binding could decrease TDP-43 biocondensate conversion to fibrilis, or maturation into irreversible aggregates. These studies are based on the paradigm that intracellular organization of RNA binding proteins into ribonucleoprotein (RNP) granules is mediated by a process of condensation or phase separation. Based on evidence emerging over the last decade, these protein and RNA-rich granules are formed via liquid-liquid phase separation (LLPS) that often show dynamic, liquid-like properties (3-5). The high concentration

of the components while retaining dynamic properties within the droplets may be essential to determine function, cellular organization and rapid response to cellular stimuli. Numerous studies also suggest that defects in LLPS homeostasis are associated with disease, such as in the case of TDP-43, FUS (Fused in sarcoma) and other RNA binding proteins linked to neurodegeneration (6-8). Specifically, conversion of the condensates into fibrils or complexes with solid-like properties may lead to the accumulation of protein aggregates associated with pathology. Our previous studies strongly suggested that biocondensate maturation is the first step in TDP-43 aggregation (1) (**Fig 2A**). We find that TDP-43 droplets fail to coalesce for up to 2 hours of incubation and, instead, form clusters or chain-like assemblies, suggesting that these complexes are more viscous and have gel or solid-like properties (**Fig 2A,B**). We asked whether association with $A(GU)_6$ RNA oligonucleotide could alter the dynamic properties of TDP-43 droplets. Consistently, addition of this RNA oligonucleotide dramatically increased the size of TDP-43 droplets compared to no RNA conditions through dynamic fusion (**Fig 2C**). The TDP-43 droplets in the presence of $A(GU)_6$ maintained liquid-like properties, as shown by fluorescence recovery after photobleaching (FRAP) (not shown). In contrast, the non-specific $A(CA)_6$ RNA or RNA binding-deficient TDP-43 mutants showed no significant changes compared to no RNA control (not shown). These results suggest that RNA binding increases the dynamic and liquid properties of TDP-43, depending on RNA sequence and specific interactions. We speculate that RNA binding prevents the conversion of TDP-43 droplets into solid-like complexes. Our work also suggests that RNA oligonucleotides may effectively block TDP-43 pathology as early as during the initial misfolding stage. This work summarized here and additional observations are included in a manuscript submitted for publication (Appendix).

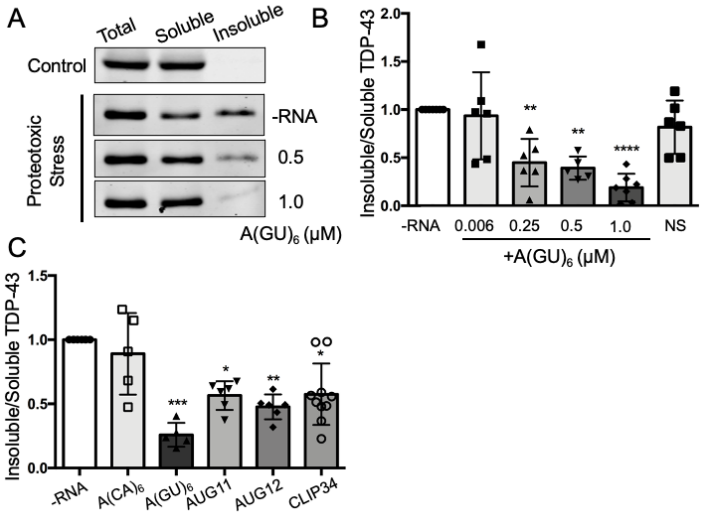


Figure 3. GU-rich RNA oligonucleotides inhibit the aggregation of TDP-43 in human cells A) Immunoblot detecting endogenous TDP-43 in total HEK293 cell lysate or following fractionation into soluble and insoluble extracts. Cells were treated with control or proteotoxic stress conditions following transfection of $A(GU)_6$ or no RNA control. **B)** Quantification of TDP-43 aggregation under proteotoxic conditions, measured as insoluble/soluble ratio from (A) at increasing $A(GU)_6$ concentration or in the presence of non-specific control RNA (NS). Analysis includes at least 5 biological independent replicates by one-way ANOVA ($F(5,31)=11.64$, $P=<0.0001$). Dunett's multiple comparisons test was used to compare treatment groups to control. **$P\leq0.01$, ****$P\leq0.0001$. **C)** Quantification of insoluble to soluble TDP-43 ratio under proteotoxic conditions in the presence of different GU-rich RNA sequences. $A(CA)_6$ RNA used as control. The values were normalized to the ratio of stress-treated cells in the absence of RNA. Analysis includes at least 5 biological independent replicates by one-way ANOVA ($F(6,39)=5.699$, $P=0.003$). Dunett's multiple comparisons test was used to compare treatment groups to control. *$P\leq0.05$, **$P\leq0.01$, ***$P\leq0.001$.

Aims 1b: Test RNA-driven inhibition of cellular TDP-43 aggregation.

We next asked whether specific RNA binding may also promote TDP-43 solubility in human cells. For this we used established assays to promote proteotoxic stress and trigger TDP-43

aggregation. Human embryonic kidney cells (HEK293) were treated with MG132 to inhibit the ubiquitin proteosomal system combined with short exposure to oxidative stress triggered by sodium arsenite. Extraction of soluble and insoluble fractions from the cell lysate showed the expected increase of TDP-43 in the insoluble fraction under proteotoxic conditions (**Fig. 3A**). Transfection of $A(GU)_6$ RNA prior to stress treatment resulted in a significant decrease of insoluble TDP-43, compared to no RNA control or non-specific RNA (NS) (**Fig. 3B**). The anti-aggregation activity of $A(GU)_6$ RNA on TDP-43 was dose-dependent. Transfection of other GU-rich RNA molecules that bind TDP-43 with apparent dissociation constants (K_d) in the nanomolar range (Table, Fig 1E) also inhibited TDP-43 aggregation significantly compared to control (**Fig. 3C**). Conversely, the non-specific $A(CA)_6$ RNA did not show a significant effect on TDP-43 aggregation relative to control. These results strongly indicate that RNA molecules that specifically bind TDP-43 are capable of acting as chaperones and prevent TDP-43 misfolding in human cells.

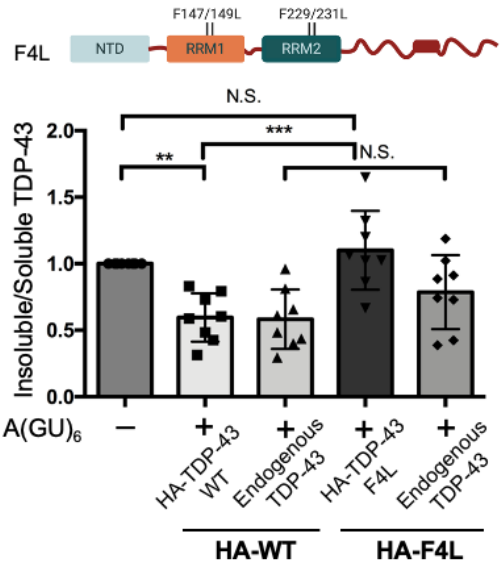


Figure 4. Specific RNA binding is necessary to prevent TDP-43 aggregation by RNA. Four site-specific mutations in the RNA binding domains (F4L) disrupt TDP-43 RNA binding activity. Quantification of TDP-43 aggregation from HEK293 cells stably expressing hemagglutinin (HA) tagged TDP-43, WT or F4L. The insoluble/soluble ratio of HA-TDP-43 transgene and endogenous TDP-43 from cells treated with proteotoxic stress, following transfection with $A(GU)_6$ RNA. Values were normalized to no RNA control. Mean of 8 biological independent replicates and analyzed by one-way ANOVA ($F(4,35)=5.863$, $P=0.001$). Sidak's multiple comparisons test was used to compare treatment groups. *$P \leq 0.05$, **$P \leq 0.01$.

To further confirm that RNA stabilizes TDP-43 solubility through specific binding, we studied cells expressing the RNA binding-deficient TDP-43 mutant, F147/149/229/231L (F4L). In this case, $(GU)_6$ treatment was not able to rescue F4L aggregation (**Fig 4**). Interestingly, we also measured greater F4L aggregation in cells not treated with RNA, compared to wild-type (not shown). Similarly, endogenous TDP-43 showed greater aggregation in F4L expressing cells, relative to WT cells. These findings suggest that the inability to bind RNA strongly impairs TDP-43 solubility. Moreover, the presence of F4L noticeably disrupts the homeostasis of normal TDP-43 expressed in the same cells, perhaps through a prion-like mechanism. Collectively, our data provides strong evidence that the chaperone function of RNA is correlated with its binding affinity to TDP-43, as predicted from our studies using purified protein.

During the design of this aim we considered the possibility that sequences that bind TDP-43 with tight binding affinity (low nanomolar range), as $(GU)_6$, may compete with TDP-43 RNA binding partners and inhibit RNA processing. To test this, we measured the effect of RNA treatment on TDP-43 autoregulatory function in cells, using well-established assays in our lab. Our preliminary data shows no significant cell toxicity under the conditions tested. Moreover, $(GU)_6$ treatment did not significantly alter TDP-43 autoregulation, suggesting that GU-rich RNA does not significantly affect physiological TDP-43 activity in cells. To further test whether RNA treatment unintendedly decreases TDP-43 function, we will analyze changes in the processing of known TDP-43 targets (9-11). In addition, we found that RNA treatment did not significantly

change TDP-43 cellular localization. Both RNA and control treated cells showed diffuse nuclear TDP-43 combined with characteristic nuclear foci and no increase in cytoplasmic detection. Furthermore, we performed initial studies to test whether $(GU)_6$ could alter the function of RNA binding proteins other than TDP-43. We surveyed the formation of ribonucleoprotein (RNP) granules and their localization in $(GU)_6$-treated cells and compared them to control treated cells. More specifically, we visualized Cajal bodies (coilin), nucleoli (fibrillarin), splicing speckles (SC35), and stress granules (TIA-1). Our results show no significant changes in RNP granule assembly or localization, suggesting that $(GU)_6$ RNA does not alter RNA binding protein behavior in general, under the conditions tested.

Aim 2–Determine whether RNA inhibits intracellular TDP-43 aggregate seeding and propagation. Recently, we showed that transfection of human cells with recombinant TDP-43 aggregates results in a 3-fold increase in cellular TDP-43 cytoplasmic aggregation relative to treatment with soluble protein (1). Indeed, additional recent studies show that frontotemporal dementia (FTD)-derived, TDP-43-positive extracts spread TDP-43 pathology in mouse brain (12). The ability of TDP-43 aggregates to spread intracellularly in prion-like fashion is a strong indication that TDP-43 inclusions are toxic and support a gain of function mechanism in pathogenesis. In this aim we examine the potential of RNA-based tools to prevent disease progression by targeting a central mechanism in the spread of TDP-43 pathology. Using our established cellular reporter, we tested whether $(GU)_6$ RNA was able to prevent propagation of TDP-43 inclusions and found that intracellular seeding triggered by pre-formed TDP-43 aggregates significantly decreased in the presence of $(GU)_6$ RNA (**Fig 5**). We have recently developed two additional models to study cellular TDP-43 aggregate seeding and spread of pathology. One approach is to analyze TDP-43 aggregate propagation in primary neurons derived from mouse brain cortex. The other technique uses recently obtained cell lines from our collaborator Marc Diamond (UT Southwestern) that are used to sense TDP-43 aggregation on the basis of Foster resonance energy transfer (FRET). We used these cell lines to detect TDP-43 aggregation and seeding using frontotemporal dementia extracts and pre-formed aggregates from purified TDP-43. Based on our promising results with the FRET sensor line, we will use these to test the effect of RNA oligonucleotide treatment on TDP-43 aggregate seeding. The advantage of this method compared to the previously developed sensor cell line is that FRET analysis may be easily adapted for medium or high throughput screening.

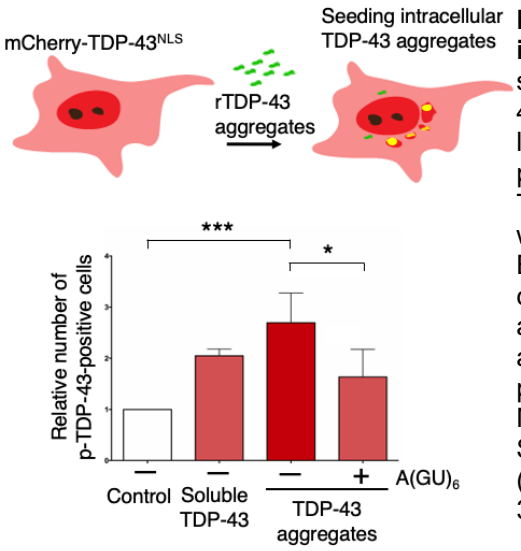


Figure 5. RNA inihibits TDP-43 intracellular seeding. HEK293 cells stably expressing mCherry tagged TDP-43, carrying mutations in the nuclear localization signal. Cells are treated with pre-formed aggregates of purified TDP-43. The seeds are internalized and colocalize with de novo cellular TDP-43 inclusions. Bottom graph shows cells treated with control, purified soluble TDP-43, TDP-43 aggregates formed in the presence and absence of $A(GU)_6$. Quantification of pTDP-43-positive cells relative to control. Mean of four independent replicates and S.D. analyzed by one-way ANOVA ($F(3,12)=12.55$, $P=5x10^{-4}$), *P=0.01, ***P= $3x10^{-4}$.

Aim 3– Use RNA to decrease TDP-43 pathology and neurotoxicity in an animal model of ALS. To determine the relevance and test the potential applicability of RNA molecules in decreasing TDP-43 pathology we applied this new approach in a mouse model of ALS. One of the few ALS mouse models that recapitulates TDP-43 pathology and neurotoxicity, as seen in human patients, is achieved by expressing the nuclear localization signal (NLS)-deficient TDP-43 mutant, TDP-43^{NLS}, in motor neurons (13). These mice, known as hTDP-43ΔNLS, express a human copy of the mutant. TDP-43^{NLS} accumulates in cytoplasmic inclusions and the mice suffer neuronal loss and a progressive ALS-like phenotype. We generated this double transgenic mouse line under "tet off" control and used these animals to evaluate the effects of TDP-43-binding RNA molecules *in vivo*.

To accomplish this, we first adapted four oligonucleotides from our *in vitro* studies for use in the *in vivo* work: Clip-34, a scrambled Clip-34 transcript, $(GU)_6$, and $(CA)_6$. Clip-34 and $(GU)_6$ both bind to TDP-43 with high affinity, while the scrambled Clip-34 and $(CA)_6$ oligonucleotides do not (**Fig 1**). After generating oligonucleotides that are tolerated at an intraventricular dose of 100 µg, we delivered these doses to hTDP-43ΔNLS mice, initiated transgene expression via doxycycline diet, and sacrificed mice two weeks into the disease process to evaluate TDP pathology. We also measured motor behavior performance on the Rotarod at baseline and weekly following transgene induction.

Interestingly, we discovered that each of the RNA oligonucleotides increased the nuclear localization of TDP-43 in motor cortical neurons two weeks into the disease process, regardless of their expected binding affinity (**Fig 6A,B**). Consistent with this improvement in TDP-43 pathology, we also observed a motor behavioral improvement in mice treated with RNA oligonucleotides compared to saline treatment (**Fig 6C**).

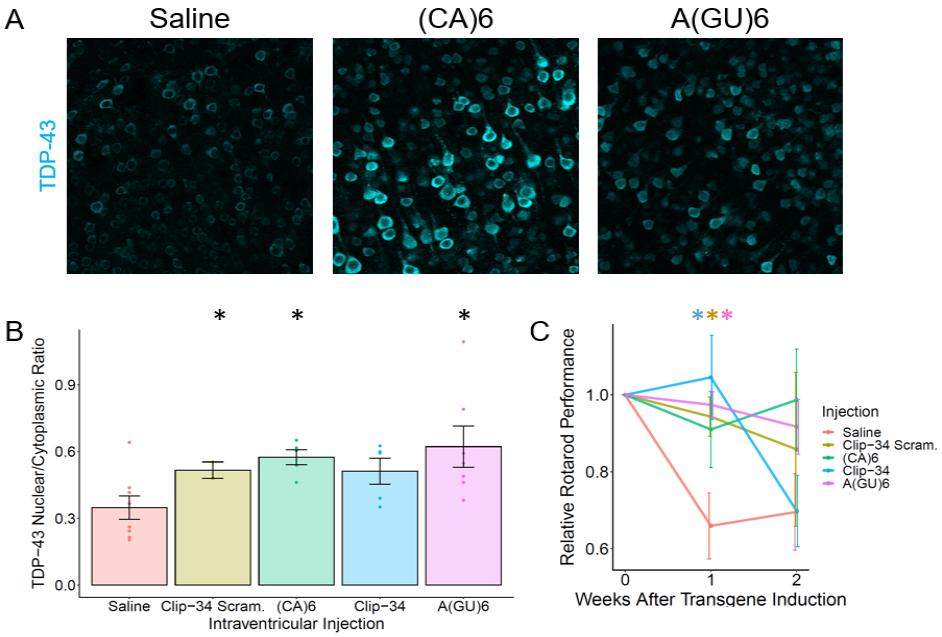


Figure 6. Injected oligonucleotides counteract TDP-43 mislocalization and toxicity *in vivo*.
A) Representative images from motor cortex of intraventricularly injected hTDP-43ΔNLS mice two weeks after transgene induction. **B)** Quantification of TDP-43 fluorescence nuclear/cytoplasmic ratio from neurons in motor cortex two weeks after transgene induction. Each data point represents the average ratio from 20 manually segmented neurons for a single mouse (n=2-8/group). **C)** Relative rotarod performance normalized to the number of seconds each mouse could remain on the accelerating Rotarod on the day of transgene induction (n=2-7/group). Error bars report standard error. Unpaired t-test saline vs. oligonucleotide, *p<0.05.

What opportunities for training and professional development has the project provided?

Nothing to report

How were the results disseminated to communities of interest?

Nothing to report

What do you plan to do during the next reporting period to accomplish the goals?

Aim 1. Establish RNA-based methods to block TDP-43 aggregation.

Our observations indicate that the ability of RNA to maintain TDP-43 solubility directly correlates with binding affinity. We will screen approximately 50 RNA oligonucleotides from two different experimental paradigms: 1) sequences will be selected based on GU-sequence composition using the already identified sequences as template; 2) sequences derived from a de novo screen using bacterial RNA pools and a synthetic RNA library. In both cases, candidate oligonucleotides will be characterized measuring TDP-43 binding affinity and TDP-43 anti-aggregation properties using our in vitro and cell-based models, as described above.

To determine whether the selected TDP-43 binding RNA oligonucleotides compete with natural transcripts and inhibit RNA processing, we will analyze changes in the processing of known TDP-43 targets. These will include those that are subject to alternative splicing or cryptic exon inclusion regulation by TDP-43. In order to test whether TDP-43 targeting RNA molecules alter the function of other RNA binding proteins we will determine whether RNA treatment significantly changes genome wide transcript levels.

Aim 2. Determine whether RNA inhibits intracellular TDP-43 aggregate seeding and propagation. The FRET sensor cell line for TDP-43 aggregation will be used to further confirm and shed light on the mechanism by which RNA molecules are able to prevent propagation of TDP-43 pathology. We have now established the method to carry out medium and high-throughput screening of RNA oligonucleotides already identified in Aim 1 and those that will be developed through further screening. Our analysis may be easily adapted for medium or high throughput screening. As part of a separate project, our lab is currently developing in vivo mouse models of TDP-43 propagation in collaboration with Dr. Albert Davis (Washington University in St. Louis). Based on our findings, we plan to test the ability of RNA to inhibit TDP-43 aggregate propagation in this in vivo model.

Aim 3. Use RNA to decrease TDP-43 pathology and neurotoxicity in a mouse model of ALS.

Given the potentially nonspecific effects of oligonucleotide administration observed in the early animal studies, we plan to introduce an additional control oligonucleotide that has been previously characterized by the Miller Lab to show minimal binding not just to TDP-43 but also to other RNA binding proteins and mRNA transcripts that may affect TDP-43 biology in neurons. In addition, we plan to refine and apply biochemical assays of TDP-43 aggregation

to our *in vivo* work, and we plan to evaluate the histological and behavioral effects of our oligonucleotide treatments at later timepoints in the disease process.

4. IMPACT

What was the impact on the development of the principal discipline(s) of the project?

This proposal tests the novel idea that RNA-based tools may be used to inhibit TDP-43 aggregation and thereby decrease pathology and loss of TDP-43 function. We are currently determining whether these methods restore TDP-43 homeostasis without affecting TDP-43 function, cellular viability and animal survival. Dr. Timothy Miller, the co-Principal Investigator in this proposal, and his team are experts in using RNA oligonucleotides as a therapeutic approach to reduce ALS and other neurodegenerative disorders in various models and in first-in-kind patient clinical trials. Upon successful completion of our project we will test the efficacy of the RNA molecules in additional animal models of ALS. Our proposed studies will determine whether RNA molecules prevent the accumulation of TDP-43 pathology and toxicity upon early treatment. In addition, future studies will ask whether RNA-based therapy is able to reverse TDP-43 pathology in the mouse models. Based on the collection of our findings, the ultimate goal of our work is to generate new RNA-based treatments for human patient clinical trials. In addition, our studies will be the first to provide evidence that RNA association with target RNA binding proteins may modulate protein homeostasis and prevent decreased activity.

The long-term impact of our proposed work will be to accelerate the development of new drugs to combat ALS in the patient population. Development of therapies will help reduce disease, suffering, and premature death caused by ALS in both the civilian and military populations.

What was the impact on other disciplines?

Nothing to report

What was the impact on technology transfer?

Nothing to report

What was the impact on society beyond science and technology?

Nothing to report

5. CHANGES/PROBLEMS:

Changes in approach and reasons for change

Nothing to report

Actual or anticipated problems or delays and actions or plans to resolve them

The award initiated shortly after the beginning of the COVID-19 pandemic, while the Ayala and Miller labs at Saint Louis University and Washington University, respectively, were locked down

under institutional regulations. As a result, in person activities that required researchers to work in the lab and considered to be non-essential were halted, and mouse colonies were reduced such that the mouse line used for this work had to be completely re-established in late 2020. All the personnel involved in the award continued to work remotely and continued to hold regular monthly meetings between the two groups. Despite these unexpected circumstances, our groups made great progress during the first year of the award, especially upon returning to work in the lab. However, there was a delay relative to our original program. Therefore, we plan to continue our studies beyond the official end date of the award, if it is deemed necessary to complete our stated goals.

Changes that had a significant impact on expenditures

Nothing to report

Significant changes in use or care of human subjects, vertebrate animals, biohazards, and/or select agents

Nothing to report

6. PRODUCTS:

Journal Publications.

Grese ZG, Bastos ACS, Mamede LD, French RL, Miller TM and Ayala YM. RNA binding controls TDP-43 phase separation through multivalent interactions while maintaining liquid properties (2021, Submitted for publication). Acknowledgement of federal support (yes).

Other publications, conference papers, and presentations.

1. Invited Seminar, Live Like Lou Foundation Seminar Series, January 2021.
2. Student talk, Hope Center for Neurological Disorders Annual Retreat, April 2021.
3. Invited Seminar, Molecular Cell Biology Department, University of Arizona, Tucson, April 2021 (Host, Dr. Daniela Zarnescu).
4. Invited Seminar, Neuroscience Seminar Series, University of Wisconsin-Milwakee, May 2021 (Host, Dr. Christopher Quinn).

7. PARTICIPANTS & OTHER COLLABORATING ORGANIZATIONS

No change.

Please see changes in other support for key personnel attached.

8. SPECIAL REPORTING REQUIREMENTS

Nothing to report

9. APPENDICES

-References

-Other support changes

-Journal publication

REFERENCES:

1. French RL, Grese ZR, Aligireddy H, Dhavale DD, Reeb AN, Kedia N, Kotzbauer PT, Bieschke J, Ayala YM. Detection of TAR DNA-binding protein 43 (TDP-43) oligomers as initial intermediate species during aggregate formation. J Biol Chem. 2019;294(17):6696-709. Epub 2019/03/03. doi: 10.1074/jbc.RA118.005889. PubMed PMID: 30824544; PMCID: PMC6497947.
2. Buratti E, Baralle FE. Characterization and functional implications of the RNA binding properties of nuclear factor TDP-43, a novel splicing regulator of CFTR exon 9. J Biol Chem. 2001;276(39):36337-43. PubMed PMID: 11470789.
3. Brangwynne CP, Eckmann CR, Courson DS, Rybarska A, Hoege C, Gharakhani J, Julicher F, Hyman AA. Germline P granules are liquid droplets that localize by controlled dissolution/condensation. Science. 2009;324(5935):1729-32. Epub 2009/05/23. doi: 10.1126/science.1172046. PubMed PMID: 19460965.
4. Feric M, Vaidya N, Harmon TS, Mitrea DM, Zhu L, Richardson TM, Kriwacki RW, Pappu RV, Brangwynne CP. Coexisting Liquid Phases Underlie Nucleolar Subcompartments. Cell. 2016;165(7):1686-97. Epub 2016/05/24. doi: 10.1016/j.cell.2016.04.047. PubMed PMID: 27212236; PMCID: 5127388.
5. Wippich F, Bodenmiller B, Trajkovska MG, Wanka S, Aebersold R, Pelkmans L. Dual specificity kinase DYRK3 couples stress granule condensation/dissolution to mTORC1 signaling. Cell. 2013;152(4):791-805. Epub 2013/02/19. doi: 10.1016/j.cell.2013.01.033. PubMed PMID: 23415227.
6. Molliex A, Temirov J, Lee J, Coughlin M, Kanagaraj AP, Kim HJ, Mittag T, Taylor JP. Phase separation by low complexity domains promotes stress granule assembly and drives pathological fibrillization. Cell. 2015;163(1):123-33. Epub 2015/09/26. doi: 10.1016/j.cell.2015.09.015. PubMed PMID: 26406374; PMCID: 5149108.
7. Patel A, Lee HO, Jawerth L, Maharana S, Jahnel M, Hein MY, Stoynov S, Mahamid J, Saha S, Franzmann TM, Pozniakovski A, Poser I, Maghelli N, Royer LA, Weigert M, Myers EW, Grill S, Drechsel D, Hyman AA, Alberti S. A Liquid-to-Solid Phase Transition of the ALS Protein FUS Accelerated by Disease Mutation. Cell. 2015;162(5):1066-77. Epub 2015/09/01. doi: 10.1016/j.cell.2015.07.047. PubMed PMID: 26317470.
8. Lin Y, Protter DS, Rosen MK, Parker R. Formation and Maturation of Phase-Separated Liquid Droplets by RNA-Binding Proteins. Molecular cell. 2015;60(2):208-19. Epub 2015/09/29. doi: 10.1016/j.molcel.2015.08.018. PubMed PMID: 26412307; PMCID: 4609299.
9. Tollervey JR, Curk T, Rogelj B, Briese M, Cereda M, Kayikci M, Konig J, Hortobagyi T, Nishimura AL, Zupunski V, Patani R, Chandran S, Rot G, Zupan B, Shaw CE, Ule J. Characterizing the RNA targets and position-dependent splicing regulation by TDP-43. Nat Neurosci. 2011;14(4):452-8. Epub 2011/03/02. doi: 10.1038/nn.2778. PubMed PMID: 21358640; PMCID: 3108889.
10. Polymenidou M, Lagier-Tourenne C, Hutt KR, Huelga SC, Moran J, Liang TY, Ling SC, Sun E, Wancewicz E, Mazur C, Kordasiewicz H, Sedaghat Y, Donohue JP, Shiue L, Bennett CF, Yeo GW, Cleveland DW. Long pre-mRNA depletion and RNA missplicing contribute to

neuronal vulnerability from loss of TDP-43. Nat Neurosci. 2011;14(4):459-68. Epub 2011/03/02. doi: 10.1038/nn.2779. PubMed PMID: 21358643; PMCID: 3094729.
11. Ling JP, Pletnikova O, Troncoso JC, Wong PC. TDP-43 repression of nonconserved cryptic exons is compromised in ALS-FTD. Science. 2015;349(6248):650-5. Epub 2015/08/08. doi: 10.1126/science.aab0983. PubMed PMID: 26250685.
12. Porta S, Xu Y, Restrepo CR, Kwong LK, Zhang B, Brown HJ, Lee EB, Trojanowski JQ, Lee VM. Patient-derived frontotemporal lobar degeneration brain extracts induce formation and spreading of TDP-43 pathology in vivo. Nat Commun. 2018;9(1):4220. Epub 2018/10/13. doi: 10.1038/s41467-018-06548-9. PubMed PMID: 30310141; PMCID: PMC6181940.
13. Walker AK, Spiller KJ, Ge G, Zheng A, Xu Y, Zhou M, Tripathy K, Kwong LK, Trojanowski JQ, Lee VM. Functional recovery in new mouse models of ALS/FTLD after clearance of pathological cytoplasmic TDP-43. Acta Neuropathol. 2015;130(5):643-60. Epub 2015/07/23. doi: 10.1007/s00401-015-1460-x. PubMed PMID: 26197969; PMCID: PMC5127391.

Previous, Current and Pending Support

Principal Investigator, Ayala, Yuna
Institution: Saint Louis University
CDMRP Log Number: AL190060, RNA-Based Approach to Decrease TDP-43 Pathology and Neurotoxicity in ALS

CURRENT SUPPORT:

1. ALS Finding a Cure and ALS Association
Start-End dates: 11/15/2016-12/31/2021
Title: Generation of a PET Tracer for TDP-43 Aggregates for ALS and FTD
Goals: This is a multiple-PI project to develop a PET Tracer for TDP-43 aggregates in ALS/FTD that could be used to study the protein's role in disease, enable more accurate diagnoses, and assess therapeutic efficacy of novel drugs.
Specific Aims/Task:
Aim 1: Develop bioassays to assess binding affinity to aggregated TDP-43
Aim 2: Identify lead compounds with high binding affinity to aggregated TDP-43 using two-pronged approach
Aim 3: Synthesis of TDP-43 targeted PET radiopharmaceuticals and assessment of radiochemistry, blood brain barrier permeability, and binding affinity to aggregated TDP-43
Aim 4: Optimization of lead TDP-43 PET radiopharmaceuticals via pharmacokinetic studies in rodent models
Aim 5: Evaluation of translational potential of TDP-43 targeted PET radiopharmaceuticals via preclinical MicroPET validation studies and analyses
Role: PI (0.01 calendar)
Total cost: \
Point of contact: Christine Collins, Grants Officer. 23 Barry Place, Stamford, CT 06902

2. Department of Defense, Congressionally Directed Medical Research Programs Amyotrophic Lateral Sclerosis Research Program Therapeutic Idea Award W81XWH2010241
Start-End dates: 07/01/2020-06/30/2022
Title: RNA-Based Approach to Decrease TDP-43 Pathology and Neurotoxicity in ALS
Goals: Test the efficacy of using RNA molecules to promote TDP-43 solubility and prevent pathology in ALS models using cell-based methods and an in vivo model of ALS.
Specific Aims/Task:
Aim 1: Establish RNA-based methods to block TDP-43 aggregation
Aim 2: Determine whether RNA inhibits intracellular TDP-43 aggregate seeding and propagation
Aim 3: Use of RNA to decrease TDP-43 pathology and neurotoxicity in a mouse model of ALS
Role: PI (2.4 calendar)
Total cost:

Point of contact: Brett Chaney, Science Officer, Brett.l.chaney.CIV@mail.mil

3. National Institutes of Health/NIA NINDS R01NS114289
Start-End dates: 02/01/2020-01/31/2025
Title: Role of oligomeric TDP-43 aggregate intermediates in ALS and frontotemporal dementia
Goals: This proposal aims to detect intermediates of TDP-43 aggregates in cells and disease and to determine the mechanisms that mediate their formation. In addition, we will test their ability to seed and propagate TDP-43 pathology in mice.
Specific Aims/Task:
Aim 1: Determine the presence of early-stage oligomers during TDP-43 aggregation in cells, in ALS and FTD
Aim 2: Determine the molecular mechanism for oligomer assembly during TDP-43 aggregation
Aim 3: Determine aggregate seeding and propagation of TDP-43 oligomers in vivo

Role: PI (4.56 calendar)
Total cost:
Point of contact: Amelie Gubitz, Program Officer, gubitza@mail.nih.gov

4. National Institutes of Health/NIA NINDS R01NS116176
Start-End dates: 04/01/2020-03/31/2025
Title: Functional and Pathological interactions of TDP-43
Goals: This is a collaboration with Nicolas Fawzi (Brown University) to uncover the structural and functional determinants that regulate TDP-43 interactions and cellular function in RNA processing. My laboratory only receives a small amount of funds through a subcontract with the goal of defining the structural requirements regulating TDP-43 RNA processing function in human cells.
Specific Aims/Task:
Aim 1: Structural basis for TDP-43 helical subdomain assembly
Aim 2: Modulation of TDP-43 CTD interactions by post-translational modifications and disease mutations
Aim 3: Structural basis for TDP-43 N-terminal region contributions to function and aggregation in disease
Role: co-PI (1.2 calendar)
Total cost:
Point of contact: Amelie Gubitz, Program Officer, gubitza@mail.nih.gov

Other Financial Support – Timothy Miller

There is no overlap between the project and any of the following Active, Pending, or Prior financially-supported projects.

ACTIVE

Research Grant (Miller, PI) 11/01/2020 – 10/31/2025 .36 Calendar
Target ALS per year
Ken Devaney, Grants Officer
P.O. Box 1598
New York, NY 10101
"Longitudinal Biofluids Core"
Major Goals: Determine biomarkers changes in cerebral spinal fluid and serum from patients with ALS.
Aim 1: Generate a biorepository of longitudinal blood (plasma, serum), CSF and urine linked to genetics and longitudinal clinical information that are made available to the research community.

Research Grant (Miller, Co-PI) 11/02/2020 – 11/01/2022 .60 Calendar
Target ALS (Miller portion)
Ken Devaney, Grants Officer
P.O. Box 1598
New York, NY 10101
"High Resolution Analysis of Neurofilament in ALS biofluids"
Major Goals: Complete in-depth discovery mass spectrometry in CSF from ALS and controls to determine if there are unique neurofilament protein signatures in ALS.
Aim 1: Identify and characterize unique neurofilament isoforms and post-translational modifications in ALS biofluids by immunoprecipitation-mass spectrometry.
Aim 2: Determine effect of therapy on neurofilament isoforms in biofluids from SOD1-ALS participants administered SOD1-lowering antisense oligonucleotides.

Research Grant (Miller, co-PI) 12/01/20 – 05/31/22 1.2 Calendar
Chan Zuckerberg Initiative (Miller portion)
Katja Brose, PhD, Program Officer
394 Pacific Ave., 2nd Floor
San Francisco, CA 94111
"*Using antisense oligonucleotides to increase mRNA translation for neurodegeneration"*
Major Goals: Determine if antisense oligonucleotides targeting the 3" UTR of mRNA transcripts can be used as a viable strategy to substantially increase protein expression.
Aim 1: Develop a screen to identify ASOs that increase expression of PGRN and TBK1.
Aim 2: Determine efficacy of candidate ASOs in PGRN and TBK1-deficient human iPSC-derived neuronal cells.

Research Grant (Miller, PI) 12/01/2020 – 11/30/2021 .60 Calendar
Rainwater Tau Consortium
Patrick Brannelly, Grants Officer
777 Main Street, Suite 2250
Fort Worth, TX 76102
"*Characterizing the impact of increased 4R tau in human astrocytes and their potential as a therapeutic target"*

Major Goals: Provide an in-depth analysis of tau protein in astrocytes and establish whether astrocytic tau may be an important target for therapeutics.
Aim 1: Evaluate efficacy of tau lowering and tau splicing in commercially available ASOs.
Aim 2: Identify if altering tau isoforms changes tau half-life in neurons.
Aim 3: Measure protein levels of tau in astrocytes.

Research Grant (Miller, Site PI) 03/01/2020 – 02/28/2022 .24 Calendar
Department of Defense
Brett Chaney, Science Officer
Congressionally Directed Medical Research Programs (CDMRP)
1077 Patchel St.
Fort Detrick, MD 21702
"RNA-Based Approach to Decrease TDP-43 Pathology and Neurotoxicity in ALS"
Major Goals: Accelerate the development of new therapeutic molecules to treat ALS by inhibiting TDP-43 pathology and decrease the associated toxicity.
Aim 1: Establish RNA-based methods to block TDP-43 aggregation.
Aim 2: Determine whether RNA inhibits intracellular TDP-43 aggregate seeding and propagation.
Aim 3: Use of RNA to decrease TDP-43 pathology and neurotoxicity in a mouse model of ALS.

Research Grant (Miller, Site PI) 04/01/2020 – 03/31/2022 .60 Calendar
Department of Defense
Jamie Shortall, Grants Officer
Assistance Agreements Group
Fort Detrick, MD 21702
"Use of High-Quality Chemical Tools to Rescue TBK1 Function and Identify Novel ATP-Competitive Targets in ALS"
Major Goals: Yield several key compounds and biological assays that target essential proteins in ALS-propagating pathways.
Aim 1: Screen kinase chemogenomic set (KCGS) to identify new ATP-binding protein targets that reduce seeding of protein aggregates.
Aim 2: Develop a TBK1-activating activation-targeting chimera (ATTAC).
Aim 3: Develop CK2 inhibitors that inhibit p62 (nucleoporin 62) phosphorylation and indirectly activate TBK1.

Research Grant (Miller, Co-I) 07/01/2019 – 06/30/2021 .24 Calendar
Hope Center for Neurological Disorders (Miller Lab portion)
Anneliese Schaefer, Grants Officer
660 S. Euclid Ave.
St. Louis, MO 63110
"Identification of Repurposed Prescription Medications as Neuroprotective Therapy for Amyotrophic Lateral Sclerosis"
Major Goals: Identify prescription medications that can be repurposed to modify the disease course for ALS.
Aim 1: Perform a population-based case-control study using 2009 Medicare data to identify medications associated with a higher or lower risk of ALS.
Aim 2: Test the two top inversely associated medications in an SOD1 G93A rodent model of ALS.

Research Grant (Miller, Co-Investigator) 09/01/2018 - 0.60 Calendar
National Institutes of Health 08/31/2021 per year
Betty Nkansah, Grants Officer (Miller) portion)
6001 Executive Blvd, Room 6200 MSC 9663

Bethesda, MD 20892
"Parallel Analysis of Transcription and Protein-DNA Interactions in Single CNS Cells"
Major Goals: To enable the parallel analysis of transcription factor binding and mRNA expression levels from tens of thousands of single cells in the brain.
Aim 1: To develop electroporation-based and viral toolkits for the delivery of self-reporting transposons to CNS cells in vivo
Aim 2: To develop a mouse genetic toolkit for delivery of self-reporting transposons.
Aim 3: To develop robust data visualization and analysis software to jointly analyze single-cell DIPbinding and mRNA expression data in the brain.

R01NS078398 (Miller, PI) 04/01/2017 – 03/31/2022 2.70 Calendar
National Institutes of Health, NINDS per year
James Washington, Grants Officer
6001 Executive Blvd., Suite 3254, MSC 9537
Bethesda, MD 20892
"Using motor neuron specific miRNA to understand and develop novel therapeutics for motor neuron disease."
Major Goals: To employ a motor neuron specific microRNA approach to define important microRNA contributions to ALS pathogenesis, provide insight into the mechanisms underlying motor neuron degeneration, and potentially develop novel therapeutic targets for ALS and other motor neuron diseases.
Aim 1: Elucidate the impact of miR-218 release on ALS disease progression through non-cell autonomous mechanisms.
Aim 2: Assess miR-218 release from MNs and presence in CSF during disease in ALS models and patients.
Aim 3: Determine whether miRNAs define susceptibility of specific motor neuron pools.

Research Grant (Miller, Co-PI) 11/15/2016 – 12/31/2021 0.48 Calendar
ALS Finding a Cure / ALS Association
Christine Collins, Grants Officer
23 Barry Place
Stamford, CT 06902
"Generation of a PET Tracer for TDP-43 Aggregates for ALS and FTD"
Major Goals: To develop a PET Tracer for TDP-43 aggregates in ALS/FTD that could be used to study the protein's role in disease, enable more accurate diagnoses, and assess therapeutic efficacy of novel drugs.
Aim 1: Develop bioassays to assess binding affinity to aggregated TDP-43
Aim 2: Identify lead compounds with high binding affinity to aggregated TDP-43 using two-pronged approach.
Aim 3: Synthesis of TDP-43 targeted PET radiopharmaceuticals and assessment of radiochemistry, blood brain barrier permeability, and binding affinity to aggregated TDP-43.
Aim 4: Optimization of lead TDP-43 PET radiopharmaceuticals via audioradiography and immunohistochemical correlations and pharmacokinetic studies in rodent models.
Aim 5: Evaluation of translational potential of TDP-43 targeted PET radiopharmaceuticals via preclinical MicroPET validation studies and analyses.

Research Grant (Miller, Site PI) 09/01/2016 – 08/31/2022 0.42 Calendar
ALS Finding a Cure / ALS Association
Christine Collins, Grants Officer
23 Barry Place
Stamford, CT 06902
"Dominantly Inherited ALS Network (DIALS)"
Major Goals: To establish a multicenter research platform to evaluate people at high risk for ALS to discover genes that rescue or prevent ALS, identify early diagnostic signs, and ultimately prevent or delay onset of ALS.

Aim 1: Provide a platform for the testing of known ALS causative genes in people at risk for familial ALS.
Aim 2: Perform longitudinal evaluation of people at risk for inherited forms of ALS, in order to define biomarkers of disease initiation (i.e. molecular, electrophysiologic, imaging) and novel measures of clinical disease onset.

PENDING

Research Grant (Miller, co-PI) 5-year project 2.4 Calendar
National Institutes of Health
Amelie Gubitz, Program Official
6001 Executive Blvd., Suite 3254, MSC 9537
Bethesda, MD 20892
"*Bedside to Bench and Back: Identifying Neuroprotective Medications for ALS Using an Innovative Reverse-Translational Approach"*
Major Goals: Identify one or more medications suitable for clinical trial by using pharmacoepidemiologic analyses to identify drug candidates and then testing them in a mouse model.
Aim 1: Enhance pharmacoepidemiological analyses by developing a new population-based study to identify candidate medications.
Aim 2: Examine motor neuron-protective action of 8-10 candidate medications derived from the above pharmacoepidemiologic analyses using a rigorous drug selection paradigm and an established mouse model of ALS.
Aim 3: Perform targeted pharmacoepidemiology and mouse model testing of cholesterol lowering medications and ALS risk and survival.

Specific RNA interactions promote TDP-43 multivalent phase separation and maintain liquid properties

Zachary R. Grese[1], Alliny C.S. Bastos[1], Lohany D. Mamede[1], Rachel L. French[1], Timothy M. Miller[2] and Yuna M. Ayala[1*]

[1]Edward Doisy Department of Biochemistry and Molecular Biology, Saint Louis University, St. Louis, MO 63104.

[2]Department of Neurology, Washington University School of Medicine, St. Louis, MO 63110.

*Corresponding author.

Abstract

TDP-43 is an RNA binding protein that forms ribonucleoprotein condensates through liquid-liquid phase separation (LLPS) and regulates gene expression through specific RNA interactions. Loss of TDP-43 protein homeostasis and dysfunction are tied to neurodegenerative disorders, mainly amyotrophic lateral sclerosis and frontotemporal dementia. Alterations of TDP-43 LLPS properties may be linked to protein aggregation. However, the mechanisms regulating TDP-43 LLPS are ill-defined, particularly how TDP-43 association with specific RNA targets regulate TDP-43 condensation remains unclear. We show that RNA binding strongly promotes TDP-43 LLPS through sequence-specific interactions. RNA-driven condensation increases with the number of adjacent TDP-43 binding sites and is also mediated by multivalent interactions involving the amino and carboxy-terminal TDP-43 domains. The physiological relevance of RNA-driven TDP-43 condensation is supported by similar observations in mammalian cellular lysate. Importantly, we find that TDP-43-RNA association maintains liquid-like properties of the condensates, which are disrupted in the presence of ALS-linked TDP-43 mutations. Altogether, RNA binding plays a central role in modulating TDP-43 condensation while maintaining protein solubility, and defects in this RNA-mediated activity may underpin TDP-43 associated pathogenesis.

INTRODUCTION

The intracellular organization of RNA binding proteins into ribonucleoprotein (RNP) granules is mediated by a process of condensation or phase separation. Based on evidence emerging over the last decade, these protein and RNA-rich granules are formed via liquid-liquid phase separation (LLPS) that often show dynamic, liquid-like properties (Brangwynne *et al*, 2009; Feric *et al*, 2016; Wippich *et al*, 2013). The high concentration of the components while retaining dynamic properties within the droplets may be essential to determine function, cellular organization and rapid response to cellular stimuli. Formation of RNP granules is mediated by multivalent interactions, including RNA binding and self-assembly through different protein domains, such as low complexity regions (Garcia-Jove Navarro *et al*, 2019; Li *et al*, 2012; Lin *et al*, 2015; Zhang *et al*, 2015). Although RNA is a fundamental component of RNP granules, how it regulates the biogenesis and metabolism of RNP condensates is not well understood (Garcia-Jove Navarro *et al.*, 2019; Zhang *et al.*, 2015). Recent studies suggest that RNA targets may modulate the LLPS properties of RNA binding proteins through specific interactions. Numerous studies also suggest that defects in LLPS homeostasis are associated with disease, such as in the case of TDP-43 (TAR DNA binding protein), FUS (Fused in sarcoma) and other RNA binding proteins linked to neurodegeneration (Lin *et al.*, 2015; Molliex *et al*, 2015; Patel *et al*, 2015). Specifically, conversion of the condensates into fibrils or complexes with solid-like properties may lead to the accumulation of protein aggregates associated with pathology. Aggregation and loss of function of TDP-43 is a hallmark of amyotrophic lateral sclerosis (ALS), frontotemporal dementia (FTD)(Neumann *et al*, 2006; Arai *et al*, 2006) and limbic-predominant age-related TDP-43 encephalopathy (LATE)(Nelson *et al*, 2019). In addition, TDP-43 inclusions are associated with multisystem proteinopathy (MSP)(Weihl *et al*, 2009) and other neurodegenerative disorders, including Alzheimer's disease (AD) and chronic traumatic encephalopathy (CTE)(McKee *et al*, 2010).

TDP-43 is a multi-domain heterogeneous ribonucleoprotein (hnRNP) whose function is essential for the regulation of hundreds of mRNA transcripts to which it binds (Polymenidou *et al*, 2011; Tollervey *et al*, 2011). The best-characterized TDP-43 function is regulation of splicing, however, TDP-43 also participates in different mechanisms of RNA processing and transport (Alami *et al*, 2014; Buratti & Baralle,

2010). For example, TDP-43 plays a more global role in gene regulation as an inhibitor of cryptic exon inclusion (Ling *et al*, 2015) and regulates the alternative polyadenylation of >1,000 genes through direct binding (Koyama *et al*, 2016; Melamed *et al*, 2019; Rot *et al*, 2017). TDP-43 shows a strong preference for binding dinucleotide guanosine and uridine (GU) RNA motifs as seen in vitro and through the identification of coding and non-coding transcripts that bind TDP-43 in mouse brain and in human cells (Polymenidou *et al.*, 2011; Tollervey *et al.*, 2011). Purified TDP-43 binds GU repeat sequences tightly through specific interactions that are evolutionarily conserved through higher eukaryotes (Ayala *et al*, 2005; Li *et al*, 2017). TDP-43 forms RNP granules in different cell types, including Cajal bodies and paraspeckles in the nucleus (Izumikawa *et al*, 2019; Modic *et al*, 2019; West *et al*, 2016) and is recruited to mRNA transport granules in neurons (Alami *et al.*, 2014). TDP-43-positive granules may form under conditions of proteotoxic stress as nuclear or cytoplasmic stress granules (Dewey *et al*, 2012; Udan-Johns *et al*, 2014). In addition, our lab showed that specific phosphorylation in RRM1 results in nucleolar localization (Li *et al.*, 2017), suggesting that posttranslational modifications may regulate TDP-43 RNP body dynamics.

To investigate the mechanisms underlying RNA-mediated assembly of TDP-43 RNP granules, which remain largely unknown, we asked whether TDP-43 LLPS properties are modulated by RNA molecules depending on sequence and number of proximal protein binding sites. We found that specific interactions of TDP-43 with RNA consisting of multiple binding sites readily promote phase separation into droplets that exhibit the liquid-like properties associated with LLPS. Moreover, we observe that specific RNA binding increases the liquid properties of TDP-43 droplets. With this experimental paradigm in place, we were also able to determine the impact of disease-associated TDP-43 mutations on RNA-mediated LLPS properties of TDP-43. We found that specific mutations reduced the liquid properties of RNA-driven TDP-43 condensates. Importantly, we found that specific RNA binding also triggered TDP-43 phase separation in mammalian cell lysate in the presence of multiple binding sites. Based on our observations, we speculate that physiological RNA recruitment of TDP-43 nucleates phase separation and, at the same time, prevents the conversion of the droplets into solid-like complexes.

Materials and Methods

Reagents were purchased from Sigma unless otherwise noted. All experiments, unless otherwise noted were performed at room temperature (approximately 22°C).

Expression and Purification of Recombinant TDP-43— Recombinant His_6-SUMO N-terminally tagged TDP-43 was expressed in BL21(DE3) *Escherichia coli* cells from the SUMO-TDP43 plasmid (pET28b(+)-SUMO-TDP43)(Li *et al.*, 2017). Mutants were generated by QuickChange site-directed mutagenesis (Agilent) using DNA oligonucleotides listed in **Supplementary Table 2**. The protocol for protein preparation was modified from previously described methods (Li *et al.*, 2017). Briefly, induction was carried out with 0.3 mM isopropyl β-D-thiogalactopyranoside (IPTG) and cells were grown at 16°C for 16 h. Cell pellets were resuspended in lysis buffer (1 M NaCl, 50 mM HEPES, pH 7.5, 2% TRITON X-100, 5% glycerol, SIGMAFAST EDTA-free protease inhibitor cocktail, 2.5 µg/ml lysozyme, 10 µg/ml DNase I, 1 mM (tris(2-carboxyethyl)phosphine)

(TCEP)). Lysates were centrifuged for 20 min at 20,000 x *g* at 4°C following sonication on ice. Protein was bound to nickel-nitrilotriacetic acid resin (McLab), and the resin was loaded into a column for purification (AKTA-Start, GE Healthcare). The column was washed with wash buffer 1 (500 mM NaCl, 50 mM HEPES, pH 7.5, 5% glycerol, 1 mM TCEP), followed by wash buffer 2 (500 mM NaCl, 50 mM HEPES, pH 7.5, 5% glycerol, 50 mM Imidazole, 1 mM TCEP), and eluted in elution buffer (500 mM NaCl, 50 mM HEPES, pH 7.5, 5% glycerol, 300 mM Imidazole, 5 mM DTT). Protein was flash frozen in liquid nitrogen and stored in aliquots at -80°C.

Oligonucleotide development— All oligonucleotides were modified with a 2'OMe group as well as a phosphorothioate backbone unless otherwise noted. Oligonucleotides were synthesized and modified by Integrated DNA Technologies (IDT).

Liquid-liquid phase separation assay— Thawed recombinant protein was centrifuged for 35 min at 98,400 x *g* at 4°C to remove any pre-formed aggregates and was diluted to the required starting concentration using elution buffer. LLPS buffer (50 mM HEPES, pH 7.5, 5% glycerol, 5 mM DTT) containing appropriate NaCl and RNA concentrations was spotted onto a Lab-Tek Chambered #1.0 borosilicate cover glass slide, followed by the addition of protein. Droplets were imaged by brightfield and

fluorescence microscopy using a Leica TCS SP5 confocal microscope with an HCX APO U-V-I 100.0x / 1.30 oil immersion objective and 2.5x digital zoom at room temperature. For experiments involving fluorescently labeled protein, recombinant protein was labeled with Oregon Green 488 or Cy3 maleimide dye (Thermo Fisher Scientific, OG-TDP-43, Cy3-TDP-43) according to manufacturer's protocol, purified with Zeba Spin columns (Thermo Fisher Scientific), and mixed with unlabeled protein in a ratio of 1:10. For experiments involving fluorescently labeled RNA, Alexa Fluor 594-labeled RNA was mixed with unlabeled RNA in a ratio of 1:10. Images were taken approximately 45 min after beginning the reaction, unless otherwise noted. OG-TDP-43 was excited using a 488 nm laser line, Cy3-TDP-43 was excited using a 514 nm laser line, and labeled RNA was excited using a 543 nm laser line. For droplet area measurements, droplet regions of interest were manually selected and analyzed using ImageJ. Fluorescent channel intensity values were universally increased within experiments by the same amount for each image, and brightfield images were linearly contrasted using Leica LAS AF software.

Fluorescence Recovery After Photobleaching (FRAP)— TDP-43 and RNA liquid droplets were first generated as described above. 10 baseline images were taken in 0.376 second intervals, and ROIs were bleached for 3.76 seconds using 30% laser power from a 488 nm laser line. 11 post-bleach images were then taken in 0.376 second intervals, followed by 4 images taken in 20 second intervals. Data points were normalized using the equation $Fr(t) = \frac{I(t)-I_{bleach}}{I_{pre}-I_{bleach}}$, where *Fr(t)* is fluorescence recovery at a given time point, *I(t)* is intensity at a given time point, I_{bleach} is the intensity immediately following bleaching, and I_{pre} is the pre-bleach intensity.

High salt droplet reversal assay— TDP-43/RNA droplets were formed as described above. As soon as droplets began to settle on the glass, high salt buffer (4 M NaCl, 50 mM HEPES, pH 7.5, 5% glycerol, 5 mM DTT) was added to a final NaCl concentration of 1.3 M in order to promote dissolution of condensates.

Turbidity assay—Thawed recombinant protein was centrifuged for 35 min at 98,400 x *g* at 4°C and was diluted to the required starting concentration using elution buffer. LLPS buffer containing appropriate RNA concentration was added to clear 96-well clear-bottom plates (Greiner Bio-One), followed by the addition of protein. Plates

were read at room temperature for 1 h using a SpectraMax i3 microplate reader (Molecular Devices). Turbidity was measured as maximum absorbance at 600 nm λ.

Measurement of light phase TDP-43 concentration— Thawed recombinant protein was centrifuged for 35 min at 98,400 x *g* at 4°C and was diluted to the required starting concentration using elution buffer. LLPS buffer containing appropriate RNA concentration was mixed with protein and incubated for 30 minutes. The samples were centrifuged at 21,000 x g for 10 minutes to pellet the dense phase. The concentration of protein in the supernatant, or light phase (C_{out}), was then measured by Bradford assay using a Nanodrop spectrophotometer.

Fluorescence Anisotropy Assay— Recombinant TDP-43 wild-type (WT) and constructs previously purified were serially diluted in a 1:2 ratio (from 75 to 0 nM) into a 300 mM NaCl, 10 mM Tris (pH 8.0), 5% glycerol, 5% sucrose, 1mM TCEP buffer solution. $A(GU)_6$ RNA labeled with fluorescein isothiocyanate (FITC) from IDT was used at a final concentration of 0.6, 1.3, 2.5 and 5 nM. The protein preparations were mixed with $A(GU)_6$-FITC, protected from light, and added in triplicate in a 384-well black flat bottom plate (Corning) protected from light. The anisotropy measurements were performed in a Biotek SYNERGY Neo2 (BioSPX) plate reader with excitation and emission wavelengths of 480 and 520 nm, respectively. To assess the binding curves, the data were fitted as previously described (Li *et al.*, 2017). Data analysis was performed using GraphPad Prism 5.

Cell Constructs— HA-mEGFP-TDP constructs were created by subcloning TDP-43 cDNA into the mEGFP-C1 vector (Addgene) using the restriction enzymes XhoI and HindIII. The resulting mEGFP-TDP-43 gene was then subcloned into the pCDNA5 (Thermo) vector using the restriction enzymes EcoRV and NotI downstream of the HA-tag.

Cell culture and induction of mEGFP-tagged TDP-43— HEK Flp-In™ 293 cells (Thermo) were grown in Dulbecco's modified Eagle's medium (DMEM) supplemented with 10% fetal bovine serum. Stable incorporation of mEGFP-TDP-43 was achieved using the pcDNA™5/FRT/TO Vector system (Thermo). Cells were plated in cell-culture treated 10-cm dishes. Expression of GFP-tagged TDP-43 protein was induced at 70% confluency by addition of 1 µg/mL tetracycline for 24 hours prior to harvesting.

Cell collection, lysis, and induction of LLPS using cell lysates— The following protocol was adapted from Freibaum et al, 2021(Freibaum *et al*, 2021). Cells were washed with PBS and pelleted by centrifugation at 300 x g for 5 minutes. PBS was aspirated and cell pellets were frozen at -80°C. Prior to use, pellets were thawed at room temperature for 2 min. 200 µl lysis buffer (50 mM HEPES, pH 7.5, 500 mM NaCl, 0.5% NP-40, 5% glycerol, 5 mM DTT, and SigmaFast EDTA-free protease inhibitor cocktail) was added to cell pellets. Pellets were lysed by pipetting up and down and transferred to Eppendorf tubes, incubated for 3 minutes at room temperature, centrifuged at 21,000 x g for 5 minutes at room temperature and the supernatant was collected. Microscopy and turbidity experiments were conducted as described above, with cell lysate as 10% by volume added as the final component.

RESULTS

RNA binding increases the liquid-like properties of TDP-43 condensates. A major question in the field is whether TDP-43 condensation necessarily promotes protein aggregation, and what factors prevent TDP-43 loss of proteostasis in the condensed phase. We and others previously showed that specific RNA binding inhibits TDP-43 aggregation (French *et al*, 2019; Mann *et al*, 2019). The chaperone-like activity of GU-rich RNA in maintaining TDP-43 solubility depends on specific interactions with the RNA binding domains (French *et al.*, 2019). Here, we explored whether RNA binding increases TDP-43 solubility during phase separation. For these studies, we established reconstitution assays using purified TDP-43. Until recently, these experiments using full-length TDP-43 have been challenging, compared to studying related proteins, such as FUS and hnRNP A1, because the condensates rapidly convert into aggregates (Molliex *et al.*, 2015). We established purification and assay conditions whereby TDP-43 formed small droplets at 150 mM salt (**Figure 1A**). These droplets failed to coalesce for up to 2 hours of incubation and formed clusters or chain-like assemblies, suggesting that these complexes are more viscous and have gel or solid-like properties. This is consistent with our previous report showing increased misfolded TDP-43 oligomeric species when the droplets were incubated for 2 hours (French *et al.*, 2019). We then asked whether association with $A(GU)_6$ RNA oligonucleotide (**Supplementary Table 1**), which strongly inhibits TDP-43 aggregation in vitro (French *et al.*, 2019), alters the dynamic

properties of TDP-43 droplets. Addition of $A(GU)_6$ RNA dramatically increased the size of TDP-43 droplets compared to no RNA conditions (**Figure 1B**). The TDP-43 droplets in the presence of $A(GU)_6$ maintained liquid-like properties, as shown by fluorescence recovery after photobleaching (FRAP) (**Supplementary Figure 1**). As additional control, we used an RNA oligonucleotide of similar length, $A(CA)_6$, which previously showed no significant binding activity for TDP-43 (Buratti & Baralle, 2001). In contrast with the GU-rich RNA molecule, the control RNA oligonucleotide did not promote TDP-43 droplet coalescence. $A(GU)_6$ is predicted to interact with one TDP-43 molecule, based on biochemical and structural studies (Ayala *et al*, 2006; Lukavsky *et al*, 2013). We tested a longer RNA sequence of GU-repeats that potentially interacts with three TDP-43 molecules, $A(GU)_{18}$ (**Supplementary Table 1**), and observed a dramatic increase in the size of TDP-43 droplets compared to those formed in the presence of $A(GU)_6$ (**Figure 1B**). Together, these data indicate that RNA is a strong modulator of TDP-43 phase separation, promoting fusion and coalescence into large droplets, depending on sequence and length. In addition, our findings suggest that GU-rich oligonucleotides promote liquid-like behavior of TDP-43 condensates. This previously unexplored function of RNA may be linked to the ability of these RNA sequences to prevent TDP-43 misfolding (French *et al.*, 2019).

To further test the role of specific RNA binding in promoting dynamic, liquid properties of TDP-43-RNA droplets, we used three RNA binding-deficient TDP-43 mutants (**Figure 1C**)(Buratti & Baralle, 2001; French *et al.*, 2019). TDP-43 is composed of two tandem RNA recognition motifs (RRMs), which are important for specific binding to RNA and single stranded DNA. Of the two RNA binding domains, RRM1 confers most of the binding affinity and sequence specificity to RNA (Buratti & Baralle, 2001; Lukavsky *et al.*, 2013). The mutations studied carry substitutions in RRM1 alone, F2L (Phe147/149Leu); mutations in RRM1 and RRM2, F4L (Phe147/149/229/231Leu); and a substitution of both RRMs with monomeric GFP (N-GFP-CTD)(French *et al.*, 2019). We measured the binding affinity, apparent dissociation constant ($K_{d,app}$), of wild-type (WT) and all the mutants for GU-repeat RNA by fluorescence anisotropy (**Supplementary Figure 2**). These assays showed 11 and 92-fold loss in GU-rich RNA binding affinity for F2L and F4L compared to WT, respectively. (**Table 1**). We were unable to measure binding in the case of N-GFP-CTD. In the absence of RNA, F2L and F4L formed small droplets that were not

significantly different from WT droplets shown in figure 1B (**Figure 1C**). However, in the presence of $A(GU)_6$ RNA, F2L formed smaller droplets and decreased coalescence, compared to WT, that were not different from those in the presence of $A(CA)_6$ RNA. Furthermore, addition of $A(GU)_6$ did not significantly alter the behavior of F4L and N-GFP-CTD, compared to no RNA and $A(CA)_6$ control, forming a mixture of small droplets and fibrillar structures. Addition of the longer $A(GU)_{18}$ RNA rescued phase separation in the case of F2L and partially recovered it in the case of F4L (**Figure 1C**). In contrast, complete substitution of the RRMs in the N-GFP-CTD chimera abolished the ability of RNA to modulate condensation even in the presence of $A(GU)_{18}$. Collectively, these results suggest that decreasing RNA-TDP-43 interactions through site-directed substitutions in RRM1/2 greatly impairs the ability of RNA composed of a single binding module, $A(GU)_6$, to promote droplet liquid-like properties. However, in the presence of RNA with multiple binding sites, which bring multiple TDP-43 molecules in close proximity, phase separation of F2L and F4L is rescued and partially recovered, respectively. However, this process is no longer possible if specific RNA binding is entirely absent, as in the case of N-GFP-CTD.

Table 1. RNA binding affinity for $A(GU)_6$ RNA

Protein	$K_{d,app}$ (nM)	$K_{d,app}^{Mut} / K_{d,app}^{WT}$ *
Wild-type (WT)	0.8 ± 0.1	1
F2L (F147/149L)	9 ± 1	11
F4L (F147/149/F229/231L)	74 ± 20	92
ΔN (a.a. 102-414)	0.7 ± 0.1	0.8
Y4R/E17R	1.7 ± 0.5	2
RRM1-2 (a.a. 102-269)	0.80 ± 0.16	1
ΔC (a.a. 1-269)	1.1 ± 0.2	1.4
K181E	3.6 ± 0.5	5
A315E	1.1 ± 0.3	1.4
A315T	0.6 ± 0.1	0.8
A321G	1.3 ± 0.2	1.6
Q331K	1.6 ± 0.3	2

M337V	2.4 ± 0.5	3
A382T	0.7 ± 0.2	0.9

*Estimated loss (>1) or gain (<1) in binding affinity relative to WT.

RNA binding to multiple sites strongly induces phase separation. Based on the results described above, we sought to further investigate how RNA sequences that recruit multiple TDP-43 molecules affect phase separation. In particular, we were interested in surveying RNA molecules representative of natural TDP-43 targets, including GU repeat tracks (Polymenidou *et al.*, 2011; Tollervey *et al.*, 2011). We previously showed that a minimum of five GU repeats is required for binding one molecule of TDP-43 and that GU repeats may be interrupted by non-specific residues without a significant loss in binding affinity (Ayala *et al.*, 2005). This was confirmed by structural studies in which binding of one TDP-43 molecule covers approximately 10-12 nucleotides through specific interactions with the RRMs (Lukavsky *et al.*, 2013). Therefore, the natural TDP-43-bound RNA sequences, consisting of long stretches of GU-rich sequences (GU-rich clusters), indicate extended regions of multiple TDP-43 binding sites (Polymenidou *et al.*, 2011; Tollervey *et al.*, 2011). Examples of these sequences include a GT repeat polymorphism (9-15 repeats) in the cystic fibrosis transmembrane conductance regulator (CFTR) modulating exon 9 splicing (Buratti *et al*, 2004) and GT-repeat stretches (10 up to 40 repeats) found in introns and 3' UTR of *Cdk6* (Ayala *et al*, 2008; Tollervey *et al.*, 2011). To explore how RNA molecules similarly composed of extended GU-rich sequences affect LLPS properties of TDP-43, we studied droplet formation at higher salt (250 mM NaCl). Under these conditions, TDP-43 does not phase separate on its own (**Figure 2A**). As seen at lower salt conditions, addition of $A(GU)_{18}$ led to the spontaneous formation of protein droplets, which entirely colocalized with RNA (**Figure 2A,** visualized with 10% fluorescently labeled RNA and protein). In contrast, we did not observe TDP-43 phase separation in the presence of heparin or a non-specific single stranded DNA (ssDNA) oligonucleotide (**Supplementary Figure 3**). We also tested the effect of ssDNA composed of GT repeats $A(GT)_{18}$, which based on previous studies, binds TDP-43 through RRM interactions with approximately 200-fold lower affinity than the analogous RNA sequence (Kitamura *et al*, 2018; Kuo *et al*, 2009). This DNA oligonucleotide did not induce TDP-43 droplet formation at concentrations that strongly promoted phase

separation in the case of $A(GU)_{18}$ (**Supplementary Figure 3**). For our studies, we used modified RNA oligonucleotides to increase stability. The modification did not alter the ability of RNA to drive TDP-43 LLPS under the conditions tested, as seen by using analogous non-modified RNA (**Supplementary Figure 3**). We tested the dynamic behavior of the $A(GU)_{18}$-mediated TDP-43 droplets to determine whether these were consistent with LLPS properties. We consistently observed spherical condensates that fused and coalesced into larger droplets (**Supplementary Movie 1**). In addition, increasing salt concentration to the pre-formed droplets dissolved the dense phase (**Supplementary Movie 2**), indicating the reversibility of the multicomponent complex.

Next, we analyzed the regulation of TDP-43 LLPS by alternative RNA sequences that bind the protein but are not composed of GU-repeats. These sequences are equivalent to those found in physiological targets. The consensus sequence found among natural TDP-43-bound RNA transcripts in human cells, AUG12 (Tollervey *et al.*, 2011)(**Figure 2B**) binds one molecule of TDP-43 (Lukavsky *et al.*, 2013). We generated an RNA oligonucleotide composed of AUG12 repeated three times, $(AUG12)_3$ (**Figure 2B**). In addition, we analyzed the effect of CLIP34, a 34-nucleotide sequence derived from the *Tardbp* 3' UTR that recruits TDP-43 during autoregulation (**Figure 2B**)(Ayala *et al*, 2011; Polymenidou *et al.*, 2011; Tollervey *et al.*, 2011). At 250 mM salt, CLIP34 triggered spontaneous TDP-43 phase separation into large droplets, similar to $A(GU)_{18}$ (**Figure 2B**). Addition of $(AUG12)_3$ also induced droplets, although these were smaller compared to those driven by $A(GU)_{18}$ and CLIP34 at similar RNA concentrations (**Figure 2B**). In contrast, an alternative RNA oligonucleotide of similar length, NS (32 nucleotides), consistently showed few small droplets mixed with fibrillar structures (**Figure 2B**). Additionally, the sequence $A(CA)_{18}$ showed no effect on TDP-43 LLPS. In all, our observations provide strong evidence that RNA-drives the formation of TDP-43 condensates exhibiting liquid-like properties. In addition, the ability to promote TDP-43 demixing is unique to specific RNA sequences that are established to bind TDP-43 specifically. These RNA oligonucleotides bind TDP-43 with high affinity in vitro and are composed of sequences commonly found among physiological targets (Ayala *et al.*, 2005; Buratti & Baralle, 2001; Polymenidou *et al.*, 2011; Tollervey *et al.*, 2011).

Next, we sought to further establish the role of GU-rich RNA as a modulator of TDP-43 phase properties. First, we observed that TDP-43 droplets grew larger as $A(GU)_{18}$ concentration increased (quantified by droplet area), suggesting that the volume of the dense phase increased as a function of RNA (**Figure 3A, B**). We also quantified the concentration of TDP-43 in the light phase (C_{out}) by Bradford protein analysis following separation of dense and light phases. We found that as the size of the droplets grew with increasing $A(GU)_{18}$ concentration, C_{out} decreased (**Figure 3C**). The highest $A(GU)_{18}$ concentration led to approximately 70% reduction of TDP-43 concentration in the light phase relative to control, in the absence of RNA. This suggests that TDP-43 accumulation in the dense phase is upregulated as a function of GU-rich RNA presence. To explore whether $A(GU)_{18}$ altered the TDP-43 phase boundary, we analyzed droplet formation at different salt concentrations as a function of $A(GU)_{18}$ concentration. At equal TDP-43 concentration, the increase in salt inhibited droplet formation regardless of RNA presence (**Figure 3D**). However, $A(GU)_{18}$ promoted droplet formation at salt concentrations which were not permissive in the absence of RNA. A schematic representation of droplet formation as a function of salt indicates a shift in the TDP-43 phase boundary driven by RNA (**Figure 3E**), suggesting a decrease in the saturation concentration (C_{sat}) of TDP-43 necessary to initiate condensation. These results are consistent with the effect of GU-rich RNA on driving TDP-43 LLPS and provide strong evidence that RNA composed of multiple binding sites modifies TDP-43 phase behavior by favoring condensation.

RNA-driven TDP-43 phase separation is modulated by the number of binding sites. We next asked whether increasing multivalent association of TDP-43 molecules on an RNA template increases protein condensation. For these experiments, we studied LLPS as a function of the number of contiguous potential TDP-43 binding sites. The concentration of GU-rich RNA oligonucleotides was modified for each sequence to maintain the number of TDP-43 binding sites constant across samples. At 250 mM NaCl, addition of $A(GU)_6$ RNA, which favors binding of one TDP-43 molecule, did not promote TDP-43 liquid droplet formation (**Figure 4A**). Small droplets started to form in the presence of $A(GU)_9$ and these grew larger as a function of GU-repeat length. Quantification showed that droplet area directly increased as the number of TDP-43 binding sites (**Figure 4B**). In addition, TDP-43

concentration in the light phase (C_{out}) decreased proportionally with greater GU-repeat number (**Figure 4C**), suggesting a corresponding increase of TDP-43 in the dense phase as the number of GU-repeats increased. We also analyzed TDP-43 LLPS by measuring turbidity in the presence of the different GU-rich RNA oligonucleotides (**Supplementary Figure 4**). In agreement with our imaging data, starting with $A(GU)_9$, turbidity increased as the length of GU repeats in the sample increased. Collectively, our observations indicate that TDP-43 condensation is strongly regulated by number of proximal RNA binding sites. These findings open avenues to investigate how different TDP-43 RNA targets, which are composed of varying numbers of binding modules, may differentially regulate protein phase separation.

RNA-driven TDP-43 phase separation is mediated by N-terminal and low complexity domain interactions. To further investigate the mechanism of TDP-43 RNA-driven phase separation, we sought to investigate whether this process is also affected by TDP-43 domains that participate in protein-protein interactions and self-assembly. TDP-43 is organized into three independently folded domains followed by a mostly disordered region at the carboxyl terminus (**Figure 5A**). These four domains all contribute to TDP-43 self-assembly and RNA processing function. The N-terminal domain (NTD) folds into a homeobox-like structure that promotes TDP-43 oligomerization (Afroz *et al*, 2017; Mompean *et al*, 2017; Wang *et al*, 2018; Wang *et al*, 2013). NTD-driven complexes are necessary for protein function in RNA processing, phase separation, and for preventing the accumulation of RNA:DNA hybrid structures (Afroz *et al.*, 2017; Mompean *et al.*, 2017; Wang *et al.*, 2018; Wang *et al.*, 2013; Wood *et al*, 2020). This region is followed by the two RRMs and the carboxy-terminal domain (CTD), which is referred to as low complexity or prion-like domain for its similarity to yeast prion domains. The CTD is a mostly disordered region that undergoes phase separation alone, suggesting that it is a major driver of full-length TDP-43 condensation (Conicella *et al*, 2016). At the same time, this domain is a primary driver of protein aggregation (Johnson *et al*, 2009) and is also where almost all ALS and FTD-linked mutations are found. We investigated droplet formation using WT, mutant and TDP-43 fragments targeting the NTD and CTD (**Figure 5A**) at 250 mM salt. In the absence of RNA none of the constructs showed phase separation (**Figure 5B**). We found that deletion of both NTD and CTD (RRM1-

2) precluded TDP-43 phase separation in the presence of $A(GU)_{30}$, in contrast to WT (**Figure 5B**). A fragment lacking the entire NTD (ΔN) or two site substitutions that prevent NTD-driven oligomerization (Y4R/E17R) (Wang *et al.*, 2018) completely blocked TDP-43 phase separation in the presence of RNA (**Figure 5B**). Similarly, RNA did not promote TDP-43 LLPS in the absence of the low complexity domain (**Figure 5B**). We measured the $K_{d,app}$ of WT and all the mutants for GU-repeat RNA (**Supplementary Figure 5, Table 1**). The values obtained were consistent with those previously measured for full-length WT and fragments, including ΔC and RRM1-2, using other methods (Ayala *et al.*, 2005; Flores *et al*, 2019; Li *et al.*, 2017). In all cases, the mutations did not significantly alter the binding affinity for GU-repeats, relative to WT. This suggests that the lack of $A(GU)_{30}$-induced droplet formation by the mutants is unlikely to be caused by reduced RNA interactions. Instead, the data indicate that binding of RRM1 and RRM2 to RNA is essential, but under the conditions tested is not sufficient to promote RNA-driven TDP-43 LLPS. The N-terminal domain oligomerization as well as CTD interactions play a major role in the RNA-mediated process, which is consistent with the importance of multivalent interactions in biomolecular condensation.

ALS-linked mutations compromise RNA-driven liquid-like behavior of TDP-43 condensates. TDP-43 phase separation has been the focus of much investigation because disruption of LLPS homeostasis may underlie pathogenesis linked to protein aggregation and loss of function in neurodegeneration (Lin *et al.*, 2015; Mackenzie *et al*, 2017; Molliex *et al.*, 2015; Patel *et al.*, 2015). To shed light on disease mechanisms we analyzed the behavior of TDP-43 mutations causative of ALS/FTD. We selected a group of these, including K181E, A315E, A315T, A321G, Q331K, M337V, and A382T to determine whether they altered RNA-driven TDP-43 condensation (Baumer *et al*, 2009; Chen *et al*, 2019; Chio *et al*, 2011; Fujita *et al*, 2011; Gitcho *et al*, 2008; Sreedharan *et al*, 2008). The recently identified K181E mutation is positioned in the linker region between RRM1 and RRM2 and was shown to increase aggregation in cells (Chen *et al.*, 2019). All the other substitutions are in the vicinity or within an evolutionarily conserved region of the CTD (a.a. 320-343) that forms a partially α-helical structure important for phase separation (Conicella *et al*, 2020; Conicella *et al.*, 2016; Schmidt & Rohatgi, 2016). In addition, we and others previously showed that some of these mutants, e.g., M337V and A315T, accelerate

TDP-43 aggregation (French *et al.*, 2019),(Conicella *et al.*, 2016; Johnson *et al.*, 2009) and increase intracellular aggregate seeding (French *et al.*, 2019). We compared RNA-driven LLPS of WT and the mutants in control conditions without RNA or in the presence of $A(GU)_{18}$ RNA at 250 mM salt. Our microscopy analyses showed no significant changes in the RNA-driven LLPS of K181E, A315E, A315T, Q331K, and A382T relative to WT (**Supplementary figure 6**). In contrast, we found that A321G and M337V strongly disrupted phase separation in the presence of $A(GU)_{18}$, compared to WT (**Figure 6A**). The A321G and M337V droplets induced by the addition of $A(GU)_{18}$ were noticeably smaller than those formed by WT and assembled in clusters without fusing into larger droplets. This is highlighted by the movie monitoring M337V droplets over time showing a stark contrast to WT behavior (**Supplementary Movies 3** and **4**). We measured the binding affinity for GU-rich RNA of all the mutations tested and did not find a significant change relative to WT (**Supplementary Fig. 7, Table 1**). Therefore, our results suggest that impaired liquid properties of the RNA-mediated M337V and A321G condensates are not caused by defects in RNA association. In addition, we tested whether M337V condensates could interact with WT and impact the liquid properties of WT RNA-mediated assemblies. We mixed equal concentrations of fluorescently labeled WT and M337V proteins in the presence of $A(GU)_{18}$ RNA. This led to the formation of both larger and small chain-like droplets that consisted of WT and M337V proteins (**Figure 6B**). These results suggest that WT and mutant TDP-43 may assemble together to form condensates, however, WT protein may not transfer liquid-like properties to M337V complexes. Instead, mutant TDP-43 was able to disrupt WT LLPS behavior. These observations may be relevant to the ALS cases affected by the M337V mutation, caused by the heterozygous substitution c. 1009A>G, which has been independently found in families in a number of countries (Rutherford *et al*, 2008; Sreedharan *et al.*, 2008; Tamaoka *et al*, 2010). Our results demonstrate that one intact copy of TDP-43 is likely insufficient to prevent the maturation of liquid RNP granules to more solid structures in these patients. The assays established for these studies shed light on mechanisms essential for TDP-43 function that may be disrupted by ALS mutations and may underpin TDP-43-linked disease. Our analysis also indicates that these mutations affect protein/gene function differently. The defects observed in the case of A321G and M337V may be caused by structural alterations that inhibit LLPS and/or result in condensates with gel or more solid-like properties. For this reason,

mutant condensates may be more likely to increase fibrilization, as observed previously (French *et al.*, 2019).

RNA promotes LLPS of TDP-43 in mammalian cell lysate. Our assays to this point had tested whether RNA could induce TDP-43 LLPS in a simplified system combining primarily purified protein and RNA. However, the cellular milieu is much more complex. We asked whether we could reconstitute RNA-driven TDP-43 condensates in an environment composed of cellular cytoplasmic and nuclear components. To this end, we established a new protocol to analyze cellular extract from HEK293 cells that stably expressed a single copy of either mEGFP-TDP-43 WT or the RNA binding-deficient mutant mEGFP-TDP-43 F4L. Our methods were adapted from recent studies by Freibaum et al., 2021 to reconstitute stress granules and nucleoli in cellular lysates (Freibaum *et al.*, 2021) . We prepared cellular lysate after inducing the expression of GFP-tagged TDP-43 and added Cy3-labeled recombinant wild-type TDP-43. In the absence of RNA, the mixture appeared homogenous and lacked visible foci (**Figure 7A**). Likewise, when $A(GU)_6$ RNA, which favors binding one TDP-43 molecule, was added, the mixture remained free of liquid droplets and showed no significant increase in turbidity compared to control (**Figure 7A, B**). However, when $A(GU)_{18}$, which consists of three potential TDP-43 binding sites, was added, spherical droplets that contained both mEGFP-labeled cellular and Cy3-labeled recombinant TDP-43 formed (**Figure 7A**). Consistently, addition of $A(GU)_{18}$ led to an almost 4-fold increase in turbidity compared to control or in the presence of $A(GU)_6$ RNA (**Figure 7B**). Unlike in our LLPS assay in the absence of cellular lysate, $A(CA)_{18}$ RNA also generated a number of droplets, albeit far fewer than $A(GU)_{18}$. A corresponding significant increase in turbidity was also seen upon mixing with $A(CA)_{18}$ RNA (**Figure 7B**), however this was 50% lower than in the presence of $A(GU)_{18}$. We hypothesize that this could be due to the increased concentration of both TDP-43 and RNA in this assay, or due to the presence of other RNA-binding proteins present in the cell lysate. Lysate from cells expressing mEGFP-TDP-43 F4L combined with purified Cy3-labeled TDP-43 F4L in the presence of $A(GU)_{18}$ showed a readily noticeable decrease in the number of droplets, compared to WT (**Figure 7A**). Correspondingly, the TDP-43 F4L lysate showed decreased turbidity relative to WT TDP-43 lysate (**Figure 7B**) under phase separation-promoting conditions. In agreement with our observations using purified

protein and RNA, these experiments show that specific TDP-43 interactions with RNA composed of multiple binding sites induces LLPS in a cellular environment. Furthermore, we show that this new technique may be used to reconstitute TDP-43 RNP granules and interrogate their regulation in the presence of other cellular components.

DISCUSSION

The self-assembly of TDP-43 plays a central role in determining protein function and cellular dynamics while at the same time, aberrant self-association may lead to protein aggregation and pathology associated with numerous neurodegenerative disorders. Our goal was to investigate the control of TDP-43 condensation by RNA molecules for their role as a principal TDP-43 interacting partner. Previous studies showed that TDP-43 LLPS is inhibited in the presence of total yeast RNA, suggesting that RNA may prevent condensation and thereby counteract aggregation (Mann *et al.*, 2019). We studied RNA molecules with specific sequence composition, which represent natural TDP-43 targets. For these studies, we used a simplified system with full-length TDP-43 unencumbered by the use of large tags or oligomerization inducing factors to promote phase separation. In contrast to previous reports, we find that RNA strongly promotes TDP-43 phase separation in a sequence and length dependent manner that is mediated by specific binding, suggesting that TDP-43 condensation may be regulated by the number of proximal binding sites on RNA targets. Our experiments in cell lysates showing that RNA composed of multiple TDP-43 binding sites promotes TDP-43 phase separation, whereas RNA composed of a single binding module does not induce TDP-43 granule formation, strongly supports the physiological relevance of this RNA-mediated function. Importantly, we show that specific interactions of the RNA binding domains with GU-rich RNA are crucial to maintain liquid properties of the TDP-43 condensates. Furthermore, our results indicate that specific TDP-43 disease-linked mutations greatly impair this function of RNA, which may help explain the connection between disease-associated mechanisms and TDP-43 homeostasis.

Our studies focused on RNA composed of sequences representative of TDP-43 targets found in cells, which are characterized by long GU-rich stretches (Polymenidou *et al.*, 2011; Tollervey *et al.*, 2011). We find that these RNA

sequences that are predicted to bind multiple TDP-43 molecules are potent modulators of TDP-43 condensation. Increasing the number of TDP-43-binding modules enhances protein condensation, as seen by the size of droplets and increased enrichment of protein in the dense phase (**Figure 4**). This process is impaired upon disruption of RNA binding using either RRM mutations (**Figure 1**), or when using RNA molecules with no measurable TDP-43 binding affinity (**Figures 1, 2**). Our findings indicate that: 1) the ability of RNA to regulate TDP-43 phase separation depends on sequence-specific interactions between the RNA binding domains of the protein and RNA; and 2) the size of the TDP-43 binding region is a strong determinant of TDP-43 LLPS. These results suggest that we may predict TDP-43 LLPS based on the sequence composition of RNA targets. Furthermore, this may provide insight into how TDP-43 function is modulated depending on whether or not phase separation is involved.

To further investigate whether the RNA-driven condensation is mediated by multivalent interactions, which characterize LLPS, we disrupted domains that mediate TDP-43 oligomerization and self-assembly. Mutations either in the amino terminal or carboxyl low complexity domain block droplet formation in the presence of RNA, under the conditions tested (**Figure 5**). In addition, the ALS-associated mutations A321G and M337V, which affect a conserved region in the CTD (Conicella *et al.*, 2020; Conicella *et al.*, 2016; Schmidt & Rohatgi, 2016), show reduced liquid properties of the RNA-mediated complexes (**Figure 6**). Like the mutant fragments, the ALS mutations do not disrupt GU-rich RNA binding affinity (**Table 1**), but impair self-assembly and accelerate aggregation (French *et al.*, 2019),(Conicella *et al.*, 2016; Johnson *et al.*, 2009). These results underscore the importance of the interactions mediated by this C-terminal region during RNA-triggered condensation. We propose a model whereby RNA acts as a scaffold bringing multiple TDP-43 molecules in close proximity. The formation of the condensed meshwork is highly dependent on N-terminal and CTD interactions, which provide a multivalent network by increasing the number of crosslinks between RNA-bound TDP-43 (**Figure 8**).

We and others have shown that RNA exerts chaperone-like functions which increase solubility of RNA binding proteins in cells (Maharana *et al*, 2018), including in the case of TDP-43 (French *et al.*, 2019; Mann *et al.*, 2019). Here, we find that RNA maintains the liquid properties within the droplets, decreasing maturation into solid-

like assemblies (**Figure 1B**). This RNA activity is dependent on specific RNA binding and RNA composed of a single TDP-43 binding site, $A(GU)_6$, is sufficient to increase the liquid properties of TDP-43 droplets (**Figure 1B**) at lower salt concentration. This observation is in agreement with our previous findings that $A(GU)_6$ is a potent inhibitor of TDP-43 aggregation using the purified protein (French *et al.*, 2019). Therefore, we postulate that the RNA-bound state stabilizes the RRMs of TDP-43 in soluble conformations preventing the initial steps of protein aggregation that we previously showed to be triggered by RRM misfolding (French *et al.*, 2019). These findings may provide insight into TDP-43 proteostasis in cells, particularly in the cytoplasm where TDP-43 pathology is predominantly found (Arai *et al.*, 2006; Neumann *et al.*, 2006). The pathological inclusions in the cytoplasm may result from decreased RNA levels in this compartment relative to the nucleus, as previously suggested (Maharana *et al.*, 2018). Thus, RNA binding and recruitment to RNP granules may play a key role in maintaining soluble TDP-43 particularly in the cytoplasm. Cytosolic stress granules, which have been viewed as crucibles for TDP-43 pathology may actually be protective in preventing TDP-43 aggregation as they accumulate high levels of RNA molecules. This is supported by findings showing that TDP-43 aggregation is increased when the protein is excluded from stress granules (Gasset-Rosa *et al*, 2019; McGurk *et al*, 2018). Based on our work, we predict that the dynamic properties and reversibility of stress granules and other ribonucleoprotein granules, such as axonal RNA transport granules (Gopal *et al*, 2017), depend on specific TDP-43-RNA interactions.

In summary, our findings provide evidence for a model in which RNA binding drives TDP-43 phase separation and that this activity is modulated by the number of proximal protein binding sites (**Figure 8**). We were able to seed TDP-43 condensation with GU-rich RNA in the presence of mammalian cellular components (**Figure 7**), highlighting the strong modulatory function of this particular RNA sequence on TDP-43 phase separation. These findings carry important implications on the mechanisms by which TDP-43 controls RNA metabolism. Furthermore, our work lays the foundation for the development of new therapeutic strategies that utilize RNA molecules to alter TDP-43 phase properties and regulate protein homeostasis.

The authors declare that they have no conflict of interests.

Acknowledgements

We thank Dr. Alessandro Vindigni for his careful and close reading of the manuscript.

Z.R.G., A.C.S.B., T.M.M. and Y.M.A. designed the study; Z.R.G. generated recombinant protein and performed the phase separation analysis. A.C.S.B. generated recombinant protein and measured RNA binding affinity. L.D.M. generated DNA constructs and mutagenesis and helped with protein purification. R.L.F. helped with the initial solubility experiments and contributed with discussion. Y.M.A. wrote the manuscript. Z.R.G., A.C.S.B., L.D.M. , R.L.F, T.M.M. and Y.M.A edited and revised the manuscript.

Funding

This work was supported in part by funding from the National Institutes of Health (NIH) National Institute for Neurological Disorders and Stroke (NINDS) and National Institute for Aging (NIA) R01 NS114289 and NINDS R56 NS105806 to Y.M.A.; the Department of Defense CDMRP/ALSRP W81XWH-20-1-0241 to Y.M.A. and T.M.M.; and the NIH/NINDS R01 NS078398 to T.M.M.

REFERENCES

Afroz T, Hock EM, Ernst P, Foglieni C, Jambeau M, Gilhespy LAB, Laferriere F, Maniecka Z, Pluckthun A, Mittl P *et al* (2017) Functional and dynamic polymerization of the ALS-linked protein TDP-43 antagonizes its pathologic aggregation. *Nat Commun* 8: 45

Alami NH, Smith RB, Carrasco MA, Williams LA, Winborn CS, Han SS, Kiskinis E, Winborn B, Freibaum BD, Kanagaraj A *et al* (2014) Axonal transport of TDP-43 mRNA granules is impaired by ALS-causing mutations. *Neuron* 81: 536-543

Arai T, Hasegawa M, Akiyama H, Ikeda K, Nonaka T, Mori H, Mann D, Tsuchiya K, Yoshida M, Hashizume Y *et al* (2006) TDP-43 is a component of ubiquitin-positive tau-negative inclusions in frontotemporal lobar degeneration and amyotrophic lateral sclerosis. *Biochem Biophys Res Commun* 351: 602-611

Ayala YM, De Conti L, Avendano-Vazquez SE, Dhir A, Romano M, D'Ambrogio A, Tollervey J, Ule J, Baralle M, Buratti E *et al* (2011) TDP-43 regulates its mRNA levels through a negative feedback loop. *EMBO J* 30: 277-288

Ayala YM, Misteli T, Baralle FE (2008) TDP-43 regulates retinoblastoma protein phosphorylation through the repression of cyclin-dependent kinase 6 expression. *Proc Natl Acad Sci U S A* 105: 3785-3789

Ayala YM, Pagani F, Baralle FE (2006) TDP43 depletion rescues aberrant CFTR exon 9 skipping. *FEBS Lett* 580: 1339-1344
Ayala YM, Pantano S, D'Ambrogio A, Buratti E, Brindisi A, Marchetti C, Romano M, Baralle FE (2005) Human, Drosophila, and C.elegans TDP43: nucleic acid binding properties and splicing regulatory function. *J Mol Biol* 348: 575-588
Baumer D, Parkinson N, Talbot K (2009) TARDBP in amyotrophic lateral sclerosis: identification of a novel variant but absence of copy number variation. *J Neurol Neurosurg Psychiatry* 80: 1283-1285
Brangwynne CP, Eckmann CR, Courson DS, Rybarska A, Hoege C, Gharakhani J, Julicher F, Hyman AA (2009) Germline P granules are liquid droplets that localize by controlled dissolution/condensation. *Science* 324: 1729-1732
Buratti E, Baralle FE (2001) Characterization and functional implications of the RNA binding properties of nuclear factor TDP-43, a novel splicing regulator of CFTR exon 9. *J Biol Chem* 276: 36337-36343
Buratti E, Baralle FE (2010) The multiple roles of TDP-43 in pre-mRNA processing and gene expression regulation. *RNA Biol* 7: 420-429
Buratti E, Brindisi A, Pagani F, Baralle FE (2004) Nuclear factor TDP-43 binds to the polymorphic TG repeats in CFTR intron 8 and causes skipping of exon 9: a functional link with disease penetrance. *Am J Hum Genet* 74: 1322-1325
Chen HJ, Topp SD, Hui HS, Zacco E, Katarya M, McLoughlin C, King A, Smith BN, Troakes C, Pastore A *et al* (2019) RRM adjacent TARDBP mutations disrupt RNA binding and enhance TDP-43 proteinopathy. *Brain* 142: 3753-3770
Chio A, Borghero G, Pugliatti M, Ticca A, Calvo A, Moglia C, Mutani R, Brunetti M, Ossola I, Marrosu MG *et al* (2011) Large proportion of amyotrophic lateral sclerosis cases in Sardinia due to a single founder mutation of the TARDBP gene. *Arch Neurol* 68: 594-598
Conicella AE, Dignon GL, Zerze GH, Schmidt HB, D'Ordine AM, Kim YC, Rohatgi R, Ayala YM, Mittal J, Fawzi NL (2020) TDP-43 alpha-helical structure tunes liquid-liquid phase separation and function. *Proc Natl Acad Sci U S A* 117: 5883-5894
Conicella AE, Zerze GH, Mittal J, Fawzi NL (2016) ALS Mutations Disrupt Phase Separation Mediated by alpha-Helical Structure in the TDP-43 Low-Complexity C-Terminal Domain. *Structure* 24: 1537-1549
Dewey CM, Cenik B, Sephton CF, Johnson BA, Herz J, Yu G (2012) TDP-43 aggregation in neurodegeneration: Are stress granules the key? *Brain research*
Feric M, Vaidya N, Harmon TS, Mitrea DM, Zhu L, Richardson TM, Kriwacki RW, Pappu RV, Brangwynne CP (2016) Coexisting Liquid Phases Underlie Nucleolar Subcompartments. *Cell* 165: 1686-1697
Flores BN, Li X, Malik AM, Martinez J, Beg AA, Barmada SJ (2019) An Intramolecular Salt Bridge Linking TDP43 RNA Binding, Protein Stability, and TDP43-Dependent Neurodegeneration. *Cell Rep* 27: 1133-1150 e1138
Freibaum BD, Messing J, Yang P, Kim HJ, Taylor JP (2021) High-fidelity reconstitution of stress granules and nucleoli in mammalian cellular lysate. *J Cell Biol* 220
French RL, Grese ZR, Aligireddy H, Dhavale DD, Reeb AN, Kedia N, Kotzbauer PT, Bieschke J, Ayala YM (2019) Detection of TAR DNA-binding protein 43 (TDP-43) oligomers as initial intermediate species during aggregate formation. *J Biol Chem* 294: 6696-6709
Fujita Y, Ikeda M, Yanagisawa T, Senoo Y, Okamoto K (2011) Different clinical and neuropathologic phenotypes of familial ALS with A315E TARDBP mutation. *Neurology* 77: 1427-1431

Garcia-Jove Navarro M, Kashida S, Chouaib R, Souquere S, Pierron G, Weil D, Gueroui Z (2019) RNA is a critical element for the sizing and the composition of phase-separated RNA-protein condensates. *Nat Commun* 10: 3230
Gasset-Rosa F, Lu S, Yu H, Chen C, Melamed Z, Guo L, Shorter J, Da Cruz S, Cleveland DW (2019) Cytoplasmic TDP-43 De-mixing Independent of Stress Granules Drives Inhibition of Nuclear Import, Loss of Nuclear TDP-43, and Cell Death. *Neuron* 102: 339-357 e337
Gitcho MA, Baloh RH, Chakraverty S, Mayo K, Norton JB, Levitch D, Hatanpaa KJ, White CL, 3rd, Bigio EH, Caselli R *et al* (2008) TDP-43 A315T mutation in familial motor neuron disease. *Ann Neurol* 63: 535-538
Gopal PP, Nirschl JJ, Klinman E, Holzbaur EL (2017) Amyotrophic lateral sclerosis-linked mutations increase the viscosity of liquid-like TDP-43 RNP granules in neurons. *Proceedings of the National Academy of Sciences of the United States of America* 114: E2466-E2475
Izumikawa K, Nobe Y, Ishikawa H, Yamauchi Y, Taoka M, Sato K, Nakayama H, Simpson RJ, Isobe T, Takahashi N (2019) TDP-43 regulates site-specific 2'-O-methylation of U1 and U2 snRNAs via controlling the Cajal body localization of a subset of C/D scaRNAs. *Nucleic Acids Res* 47: 2487-2505
Johnson BS, Snead D, Lee JJ, McCaffery JM, Shorter J, Gitler AD (2009) TDP-43 is intrinsically aggregation-prone, and amyotrophic lateral sclerosis-linked mutations accelerate aggregation and increase toxicity. *The Journal of biological chemistry* 284: 20329-20339
Kitamura A, Shibasaki A, Takeda K, Suno R, Kinjo M (2018) Analysis of the substrate recognition state of TDP-43 to single-stranded DNA using fluorescence correlation spectroscopy. *Biochem Biophys Rep* 14: 58-63
Koyama A, Sugai A, Kato T, Ishihara T, Shiga A, Toyoshima Y, Koyama M, Konno T, Hirokawa S, Yokoseki A *et al* (2016) Increased cytoplasmic TARDBP mRNA in affected spinal motor neurons in ALS caused by abnormal autoregulation of TDP-43. *Nucleic acids research* 44: 5820-5836
Kuo PH, Doudeva LG, Wang YT, Shen CK, Yuan HS (2009) Structural insights into TDP-43 in nucleic-acid binding and domain interactions. *Nucleic acids research* 37: 1799-1808
Li P, Banjade S, Cheng HC, Kim S, Chen B, Guo L, Llaguno M, Hollingsworth JV, King DS, Banani SF *et al* (2012) Phase transitions in the assembly of multivalent signalling proteins. *Nature* 483: 336-340
Li W, Reeb AN, Lin B, Subramanian P, Fey EE, Knoverek CR, French RL, Bigio EH, Ayala YM (2017) Heat Shock-induced Phosphorylation of TAR DNA-binding Protein 43 (TDP-43) by MAPK/ERK Kinase Regulates TDP-43 Function. *The Journal of biological chemistry* 292: 5089-5100
Lin Y, Protter DS, Rosen MK, Parker R (2015) Formation and Maturation of Phase-Separated Liquid Droplets by RNA-Binding Proteins. *Molecular cell* 60: 208-219
Ling JP, Pletnikova O, Troncoso JC, Wong PC (2015) TDP-43 repression of nonconserved cryptic exons is compromised in ALS-FTD. *Science* 349: 650-655
Lukavsky PJ, Daujotyte D, Tollervey JR, Ule J, Stuani C, Buratti E, Baralle FE, Damberger FF, Allain FH (2013) Molecular basis of UG-rich RNA recognition by the human splicing factor TDP-43. *Nature structural & molecular biology*
Mackenzie IR, Nicholson AM, Sarkar M, Messing J, Purice MD, Pottier C, Annu K, Baker M, Perkerson RB, Kurti A *et al* (2017) TIA1 Mutations in Amyotrophic Lateral Sclerosis and Frontotemporal Dementia Promote Phase Separation and Alter Stress Granule Dynamics. *Neuron* 95: 808-816 e809

Maharana S, Wang J, Papadopoulos DK, Richter D, Pozniakovsky A, Poser I, Bickle M, Rizk S, Guillen-Boixet J, Franzmann TM *et al* (2018) RNA buffers the phase separation behavior of prion-like RNA binding proteins. *Science* 360: 918-921
Mann JR, Gleixner AM, Mauna JC, Gomes E, DeChellis-Marks MR, Needham PG, Copley KE, Hurtle B, Portz B, Pyles NJ *et al* (2019) RNA Binding Antagonizes Neurotoxic Phase Transitions of TDP-43. *Neuron*
McGurk L, Gomes E, Guo L, Mojsilovic-Petrovic J, Tran V, Kalb RG, Shorter J, Bonini NM (2018) Poly(ADP-Ribose) Prevents Pathological Phase Separation of TDP-43 by Promoting Liquid Demixing and Stress Granule Localization. *Mol Cell* 71: 703-717 e709
McKee AC, Gavett BE, Stern RA, Nowinski CJ, Cantu RC, Kowall NW, Perl DP, Hedley-Whyte ET, Price B, Sullivan C *et al* (2010) TDP-43 proteinopathy and motor neuron disease in chronic traumatic encephalopathy. *J Neuropathol Exp Neurol* 69: 918-929
Melamed Z, Lopez-Erauskin J, Baughn MW, Zhang O, Drenner K, Sun Y, Freyermuth F, McMahon MA, Beccari MS, Artates JW *et al* (2019) Premature polyadenylation-mediated loss of stathmin-2 is a hallmark of TDP-43-dependent neurodegeneration. *Nat Neurosci* 22: 180-190
Modic M, Grosch M, Rot G, Schirge S, Lepko T, Yamazaki T, Lee FCY, Rusha E, Shaposhnikov D, Palo M *et al* (2019) Cross-Regulation between TDP-43 and Paraspeckles Promotes Pluripotency-Differentiation Transition. *Mol Cell* 74: 951-965 e913
Molliex A, Temirov J, Lee J, Coughlin M, Kanagaraj AP, Kim HJ, Mittag T, Taylor JP (2015) Phase separation by low complexity domains promotes stress granule assembly and drives pathological fibrillization. *Cell* 163: 123-133
Mompean M, Romano V, Pantoja-Uceda D, Stuani C, Baralle FE, Buratti E, Laurents DV (2017) Point mutations in the N-terminal domain of transactive response DNA-binding protein 43 kDa (TDP-43) compromise its stability, dimerization, and functions. *The Journal of biological chemistry* 292: 11992-12006
Nelson PT, Dickson DW, Trojanowski JQ, Jack CR, Boyle PA, Arfanakis K, Rademakers R, Alafuzoff I, Attems J, Brayne C *et al* (2019) Limbic-predominant age-related TDP-43 encephalopathy (LATE): consensus working group report. *Brain*
Neumann M, Sampathu DM, Kwong LK, Truax AC, Micsenyi MC, Chou TT, Bruce J, Schuck T, Grossman M, Clark CM *et al* (2006) Ubiquitinated TDP-43 in frontotemporal lobar degeneration and amyotrophic lateral sclerosis. *Science* 314: 130-133
Patel A, Lee HO, Jawerth L, Maharana S, Jahnel M, Hein MY, Stoynov S, Mahamid J, Saha S, Franzmann TM *et al* (2015) A Liquid-to-Solid Phase Transition of the ALS Protein FUS Accelerated by Disease Mutation. *Cell* 162: 1066-1077
Polymenidou M, Lagier-Tourenne C, Hutt KR, Huelga SC, Moran J, Liang TY, Ling SC, Sun E, Wancewicz E, Mazur C *et al* (2011) Long pre-mRNA depletion and RNA missplicing contribute to neuronal vulnerability from loss of TDP-43. *Nat Neurosci* 14: 459-468
Rot G, Wang Z, Huppertz I, Modic M, Lence T, Hallegger M, Haberman N, Curk T, von Mering C, Ule J (2017) High-Resolution RNA Maps Suggest Common Principles of Splicing and Polyadenylation Regulation by TDP-43. *Cell Rep* 19: 1056-1067
Rutherford NJ, Zhang YJ, Baker M, Gass JM, Finch NA, Xu YF, Stewart H, Kelley BJ, Kuntz K, Crook RJ *et al* (2008) Novel mutations in TARDBP (TDP-43) in patients with familial amyotrophic lateral sclerosis. *PLoS Genet* 4: e1000193

Schmidt HB, Rohatgi R (2016) In Vivo Formation of Vacuolated Multi-phase Compartments Lacking Membranes. *Cell Rep* 16: 1228-1236
Sreedharan J, Blair IP, Tripathi VB, Hu X, Vance C, Rogelj B, Ackerley S, Durnall JC, Williams KL, Buratti E *et al* (2008) TDP-43 mutations in familial and sporadic amyotrophic lateral sclerosis. *Science* 319: 1668-1672
Tamaoka A, Arai M, Itokawa M, Arai T, Hasegawa M, Tsuchiya K, Takuma H, Tsuji H, Ishii A, Watanabe M *et al* (2010) TDP-43 M337V mutation in familial amyotrophic lateral sclerosis in Japan. *Intern Med* 49: 331-334
Tollervey JR, Curk T, Rogelj B, Briese M, Cereda M, Kayikci M, Konig J, Hortobagyi T, Nishimura AL, Zupunski V *et al* (2011) Characterizing the RNA targets and position-dependent splicing regulation by TDP-43. *Nat Neurosci* 14: 452-458
Udan-Johns M, Bengoechea R, Bell S, Shao J, Diamond MI, True HL, Weihl CC, Baloh RH (2014) Prion-like nuclear aggregation of TDP-43 during heat shock is regulated by HSP40/70 chaperones. *Human molecular genetics* 23: 157-170
Wang A, Conicella AE, Schmidt HB, Martin EW, Rhoads SN, Reeb AN, Nourse A, Ramirez Montero D, Ryan VH, Rohatgi R *et al* (2018) A single N-terminal phosphomimic disrupts TDP-43 polymerization, phase separation, and RNA splicing. *The EMBO journal*
Wang YT, Kuo PH, Chiang CH, Liang JR, Chen YR, Wang S, Shen JC, Yuan HS (2013) The truncated C-terminal RNA recognition motif of TDP-43 protein plays a key role in forming proteinaceous aggregates. *J Biol Chem* 288: 9049-9057
Weihl CC, Pestronk A, Kimonis VE (2009) Valosin-containing protein disease: inclusion body myopathy with Paget's disease of the bone and fronto-temporal dementia. *Neuromuscul Disord* 19: 308-315
West JA, Mito M, Kurosaka S, Takumi T, Tanegashima C, Chujo T, Yanaka K, Kingston RE, Hirose T, Bond C *et al* (2016) Structural, super-resolution microscopy analysis of paraspeckle nuclear body organization. *J Cell Biol* 214: 817-830
Wippich F, Bodenmiller B, Trajkovska MG, Wanka S, Aebersold R, Pelkmans L (2013) Dual specificity kinase DYRK3 couples stress granule condensation/dissolution to mTORC1 signaling. *Cell* 152: 791-805
Wood M, Quinet A, Lin YL, Davis AA, Pasero P, Ayala YM, Vindigni A (2020) TDP-43 dysfunction results in R-loop accumulation and DNA replication defects. *J Cell Sci* 133
Zhang H, Elbaum-Garfinkle S, Langdon EM, Taylor N, Occhipinti P, Bridges AA, Brangwynne CP, Gladfelter AS (2015) RNA Controls PolyQ Protein Phase Transitions. *Molecular cell* 60: 220-230

FIGURE LEGENDS

Figure 1. RNA binding promotes liquid-like properties of TDP-43 in the dense phase. A) Liquid droplets formed by purified TDP-43 at 150 mM salt observed by brightfield microscopy at different time points. B) TDP-43 droplets without RNA control or in the presence of different RNA oligonucleotide sequences (8 μM), (Supplementary Table 1) at 150 mM NaCl. C) RNA binding-deficient TDP-43 mutants generated by site-directed substitutions in RRM1 (F2L) or in both RRM domains (F4L) and substitution of RRM1 and RRM2 with monomeric GFP (N-GFP-C). Phase separation of the mutants without added RNA (control) or in the presence $A(GU)_6$ (8 μM), $A(GU)_{18}$ (2.6 μM), or $A(CA)_6$ (8 μM) at 150 mM NaCl. Representative

images for 3 independent experiments with 2 different protein preparations. Scale bars, 10 μm.

Figure 2. RNA composed of multiple binding sites potently induces TDP-43 phase separation. A) Droplets observed by brightfield and fluorescence microscopy when Oregon green labeled TDP-43 was mixed with no RNA control or Alexa 594-labeled $A(GU)_{18}$ RNA at 250 mM salt. B) Description of RNA oligonucleotide sequences composed of multiple TDP-43 binding sites, $A(GU)_{18}$, CLIP34 and $(AUG12)_3$, NS, or $A(CA)_{18}$ at 250 mM NaCl. Sequence in different colors separates regions that accommodate one TDP-43 molecule, if known. NS, non-specific control RNA. TDP-43 droplets in the presence of the different RNA sequences. In all panels, TDP-43 and RNA oligonucleotide concentration is 4 μM and 3.9 μM, respectively. Scale bars, 10 μm.

Figure 3. RNA with multiple binding sites modulates TDP-43 phase properties. A) Liquid droplets observed by brightfield and fluorescence microscopy when Oregon green labeled TDP-43 (4 μM, 10% labeled protein) was mixed with no RNA control or increasing $A(GU)_{18}$ RNA concentration at 250 mM salt. Scale bars, 10 μm. B) Area of droplets plotted at different $A(GU)_{18}$ concentrations. Mean and SD of >150 droplets from 3 independent experiments and 2 different protein preparations. C) TDP-43 concentration in the light phase measured as a function of $A(GU)_{18}$ concentration measured by Bradford protein assay. Mean and SD from 4 independent experiments and 2 different preparations. D) Phase separation of TDP-43 (4 μM) at increasing salt concentration without RNA or in the presence of increasing $A(GU)_{18}$ concentration. Scale bars, 10 μm. E) Phase diagram derived from panel E, denoting either no droplets or droplet formation for each condition.

Figure 4. TDP-43 phase separation is regulated by the number of binding sites on RNA. A) TDP-43 droplets observed by brightfield and fluorescence microscopy when Oregon green labeled TDP-43 (4 μM, 10% labeled protein) was mixed with no RNA control or GU-repeat RNA oligonucleotides of increasing length at 250 mM salt. As indicated, RNA concentration varied to maintain the concentration of TDP-43 binding sites constant. Scale bars, 10 μm. B) The plot shows droplet area quantified as a function of GU-repeat length. Mean and SD of >300 droplets from 3 independent experiments and 3 different protein preparations. C) TDP-43 concentration in the light phase (C_{out}) as a function of GU-repeat length quantified by Bradford protein assay. Mean and SD from 5 independent experiments and 2 different protein preparations.

Figure 5. RNA-induced phase separation requires multivalent interactions mediated by TDP-43 domains. A) Full-length TDP-43, mutant, and deletion fragments targeting regions that mediate self-assembly. Amino acid residue positions are indicated for each. B) Phase separation of full-length and TDP-43 variants (4 μM) mixed with $A(GU)_{30}$ RNA (0.8 μM) or no RNA control at 250 mM NaCl observed by brightfield microscopy. Representative images for 3 independent experiments with 2 different protein preparations. Scale bars, 10 μm.

Figure 6. ALS-linked TDP-43 mutations A321G and M337V impair RNA-driven phase separation. A) Single site amino acid substitutions associated with ALS A321G and M337V are part of a highly conserved region and partially α-helical

structure in the C-terminal domain. Droplets formed by TDP-43 wild-type (WT), A321G and M337V (4 μM) observed by brightfield microscopy in the presence of no RNA control or $A(GU)_{18}$ RNA (3.9 μM) at 250 mM NaCl. B) Phase separation of WT (4 μM, 10% Oregon green-labeled protein) and M337V (4 μM, 10% Cy-3-labeled protein) observed by brightfield and fluorescence microscopy in the presence of $A(GU)_{18}$ (3.9 μM) at 250 mM NaCl. The middle panel shows mixing of these WT (2 μM) and M337V (2 μM) samples. Representative images for 3 independent experiments from 2 protein preparations. Scale bars, 10 μm.

Figure 7. GU-rich RNA promotes TDP-43 phase separation in a cellular lysate. A) TDP-43 droplet formation in lysate prepared from HEK 293 cells expressing a mEGFP-tagged copy of either wild-type (WT) or F147/149/229/231L (F4L) TDP-43. Purified and labeled WT or F4L TDP-43 was added to the cellular lysate (5.3 μM, 10% Cy3-labeled protein) in the presence of $A(GU)_6$ (22.8 μM), $A(CA)_{18}$ (7.6 μM), $A(GU)_{18}$ (7.6 μM), or no RNA control. Droplets were imaged by brightfield and fluorescence microscopy. Representative images for 3 independent experiments from 2 protein preparations. Scale bars, 10 μm. B) LLPS measured by turbidity in the same experimental conditions as panel A. Mean and SD of 5 replicates from 3 independent experiments from 2 protein preparations. Analyzed by one-way ANOVA ($F(7,32)=165.8$, $P<0.0001$). Sidak's multiple comparisons test was used to compare selected groups. ***$P\leq0.001$, ****$P\leq0.0001$.

Figure 8. RNA binding is a key driver of TDP-43 phase separation maintaining liquid properties of the dense state. A) Binding of RNA promotes liquid properties of TDP-43 condensates, as shown by the fusion of droplets into larger droplets. This fluidity is impaired by the loss of RNA binding affinity or disease-linked mutations that alter phase separation, such as M337V and A321G, which could explain increased TDP-43 aggregation. B) RNA molecules that accommodate multiple TDP-43 molecules provide a scaffold and increase multivalent interactions, including N-and C-terminal domains, creating a meshwork that results in phase separation.

Fig. 1

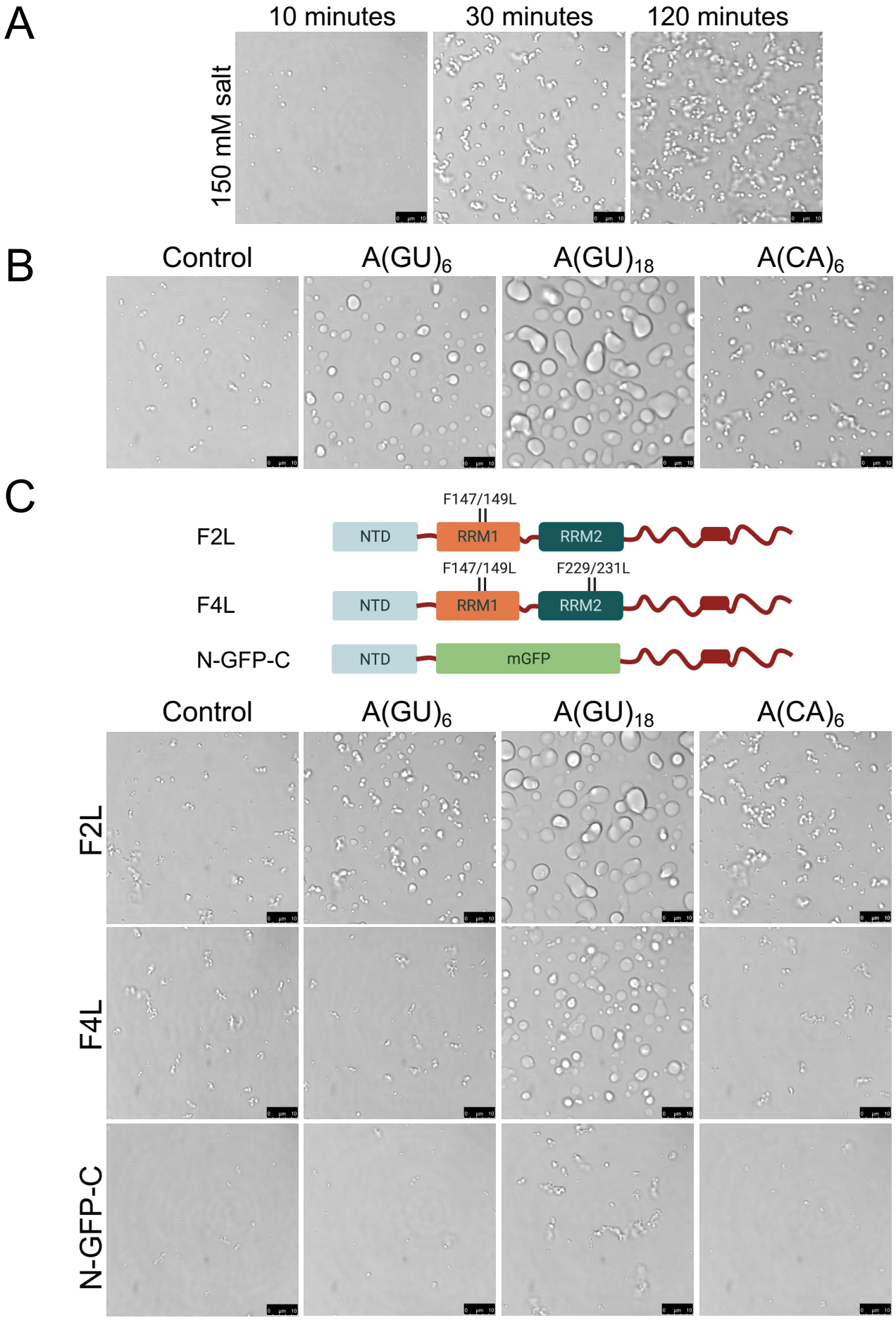
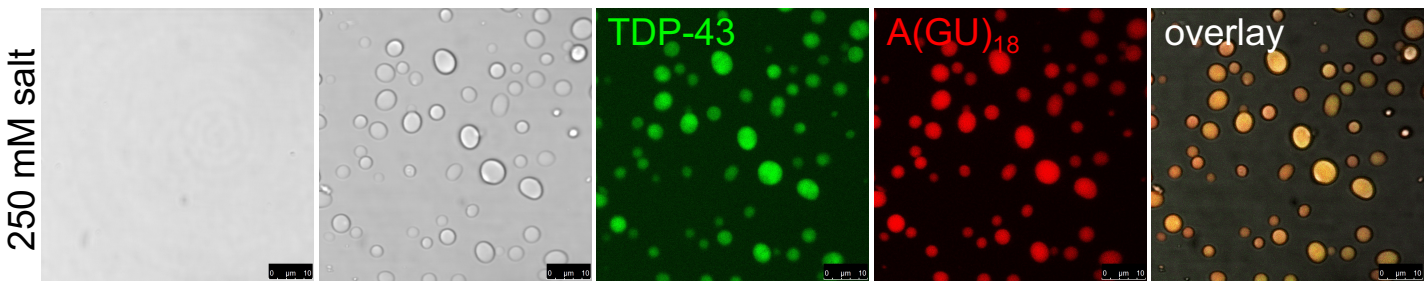

A
10 minutes
30 minutes
120 minutes
150 mM salt
B
Control
A(GU)6
A(GU)18
A(CA)6
C
F147/149L
F2L
NTD
RRM1
RRM2
F147/149L
F229/231L
F4L
NTD
RRM1
RRM2
N-GFP-C
NTD
mGFP
Control
A(GU)6
A(GU)18
A(CA)6
F2L
F4L
N-GFP-C

Fig. 2

A



B

Name	RNA oligonucleotide sequence (5'-3')
$A(GU)_{18}$	AGUGUGUGUGUGUGUGUGUGUGUGUGUGUGUGUGU
CLIP34	GAGAGAGCGCGUGCAGAGACUUGGUGGUGCAUAA
$(AUG12)_3$	GUGUGAAUGAAUGUGUGAAUGAAUGUGUGAAUGAAU
NS	CGCGACGGACGGAAAGACCCCUAUCCGUCGCG
$A(CA)_{18}$	ACACACACACACACACACACACACACACACACACACA

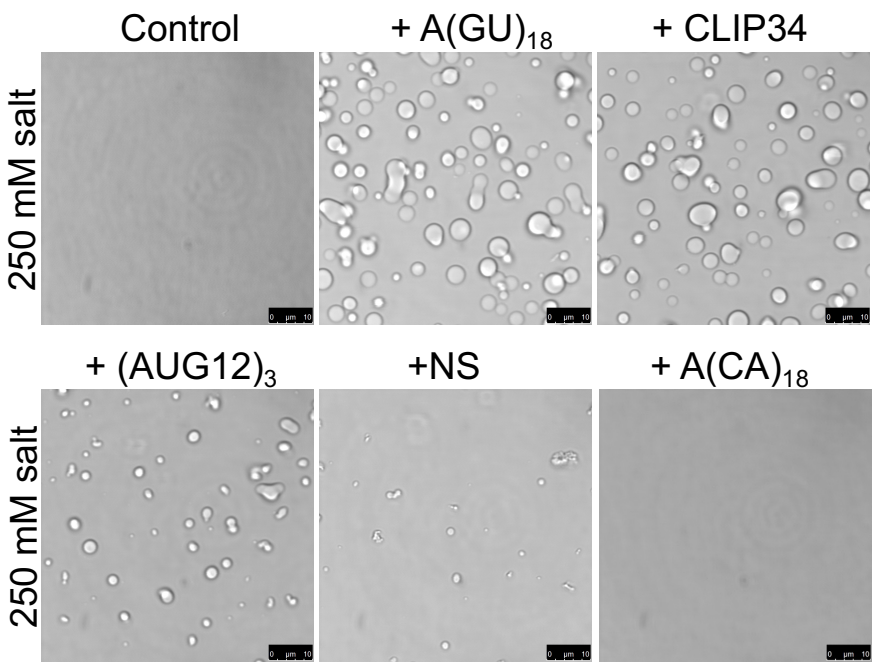


Fig. 3

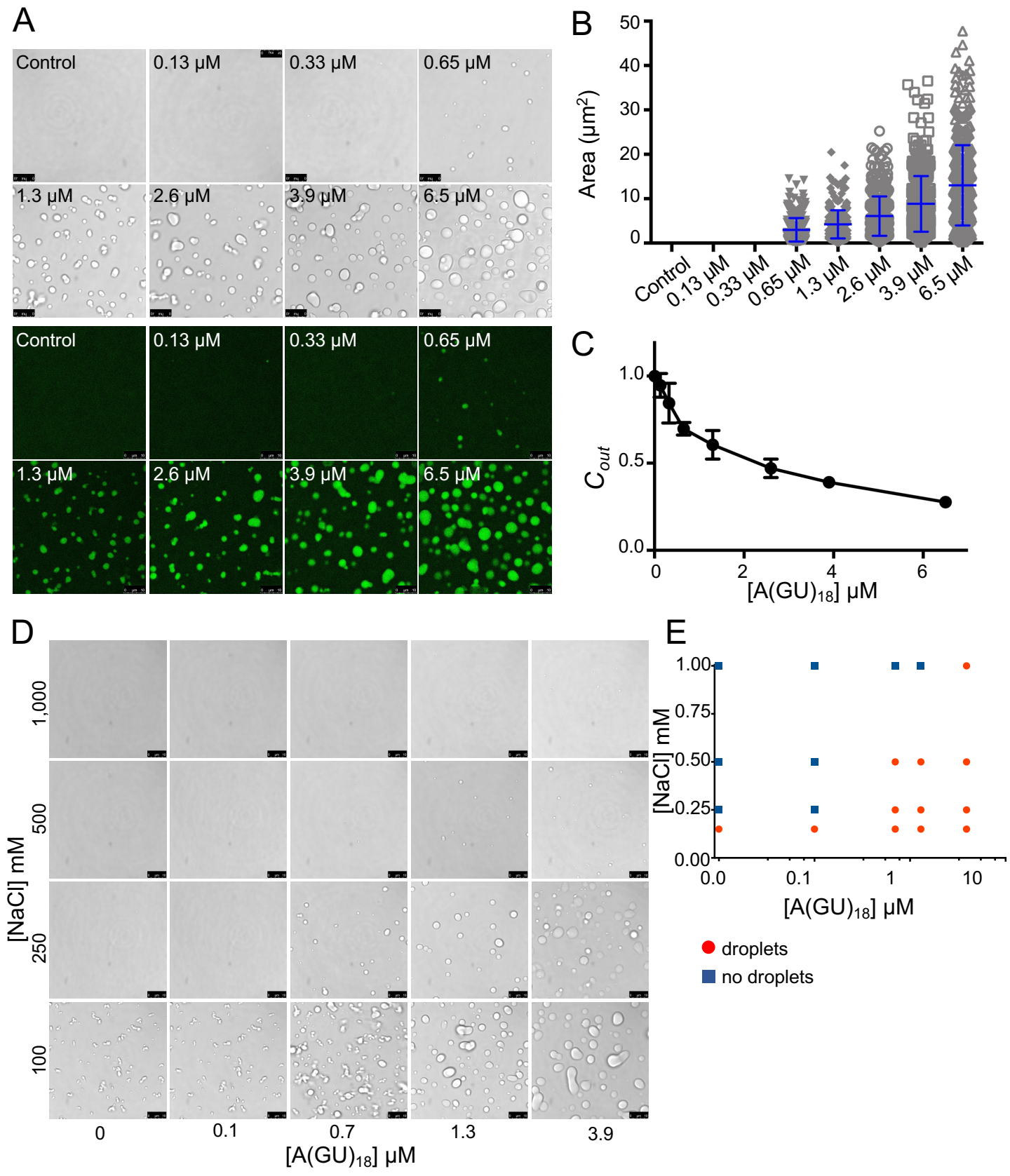

A
Control
0.13 μM
0.33 μM
0.65 μM
1.3 μM
2.6 μM
3.9 μM
6.5 μM
B
Area (μm²)
50
40
30
20
10
0
Control
0.13 μM
0.33 μM
0.65 μM
1.3 μM
2.6 μM
3.9 μM
6.5 μM
C
C_{out}
1.0
0.5
0.0
0
2
4
6
[A(GU)18] μM
D
[NaCl] mM
1,000
500
250
100
0
0.1
0.7
1.3
3.9
[A(GU)18] μM
E
[NaCl] mM
1.00
0.75
0.50
0.25
0.00
0.0
0.1
1
10
[A(GU)18] μM
droplets
no droplets

Fig. 4

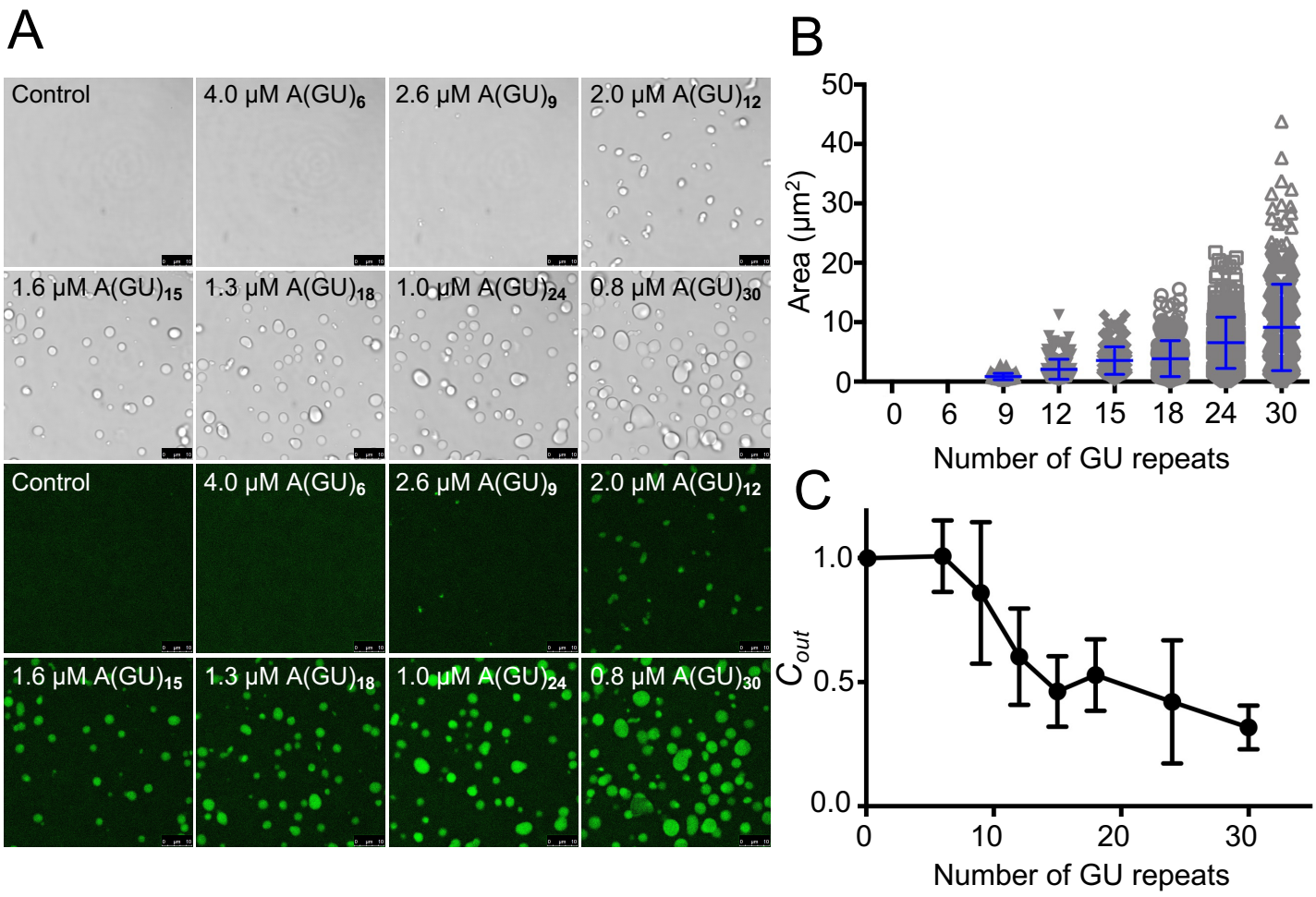
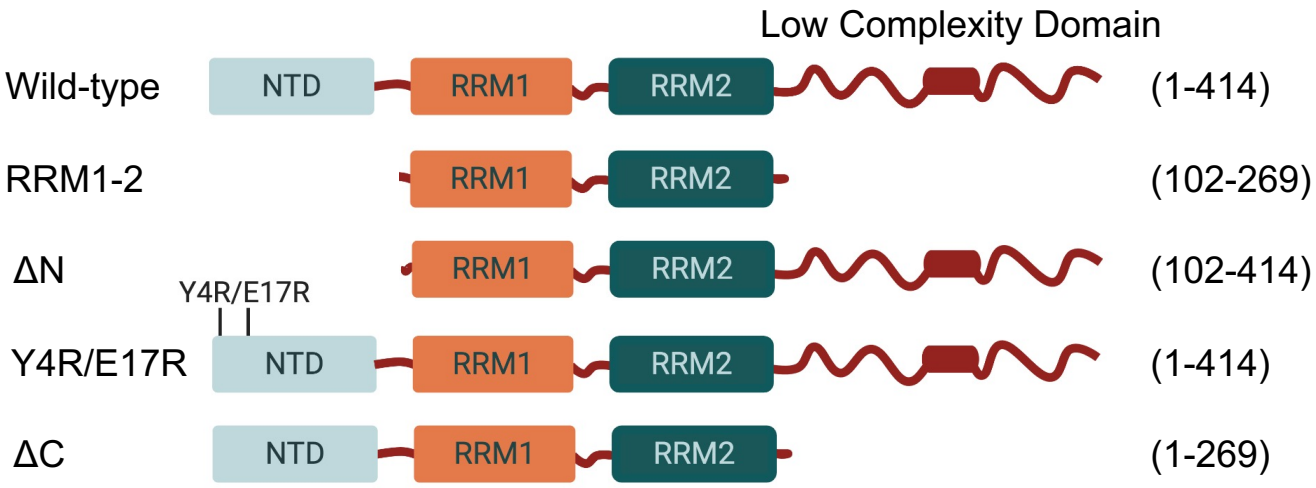

A
Control
4.0 μM A(GU)6
2.6 μM A(GU)9
2.0 μM A(GU)12
1.6 μM A(GU)15
1.3 μM A(GU)18
1.0 μM A(GU)24
0.8 μM A(GU)30
Control
4.0 μM A(GU)6
2.6 μM A(GU)9
2.0 μM A(GU)12
1.6 μM A(GU)15
1.3 μM A(GU)18
1.0 μM A(GU)24
0.8 μM A(GU)30
B
Area (μm2)
50
40
30
20
10
0
0 6 9 12 15 18 24 30
Number of GU repeats
C
Cout
1.0
0.5
0.0
0 10 20 30
Number of GU repeats

Fig. 5

A


Low Complexity Domain
Wild-type
NTD
RRM1
RRM2
(1-414)
RRM1-2
RRM1
RRM2
(102-269)
ΔN
RRM1
RRM2
(102-414)
Y4R/E17R
Y4R/E17R
NTD
RRM1
RRM2
(1-414)
ΔC
NTD
RRM1
RRM2
(1-269)

B

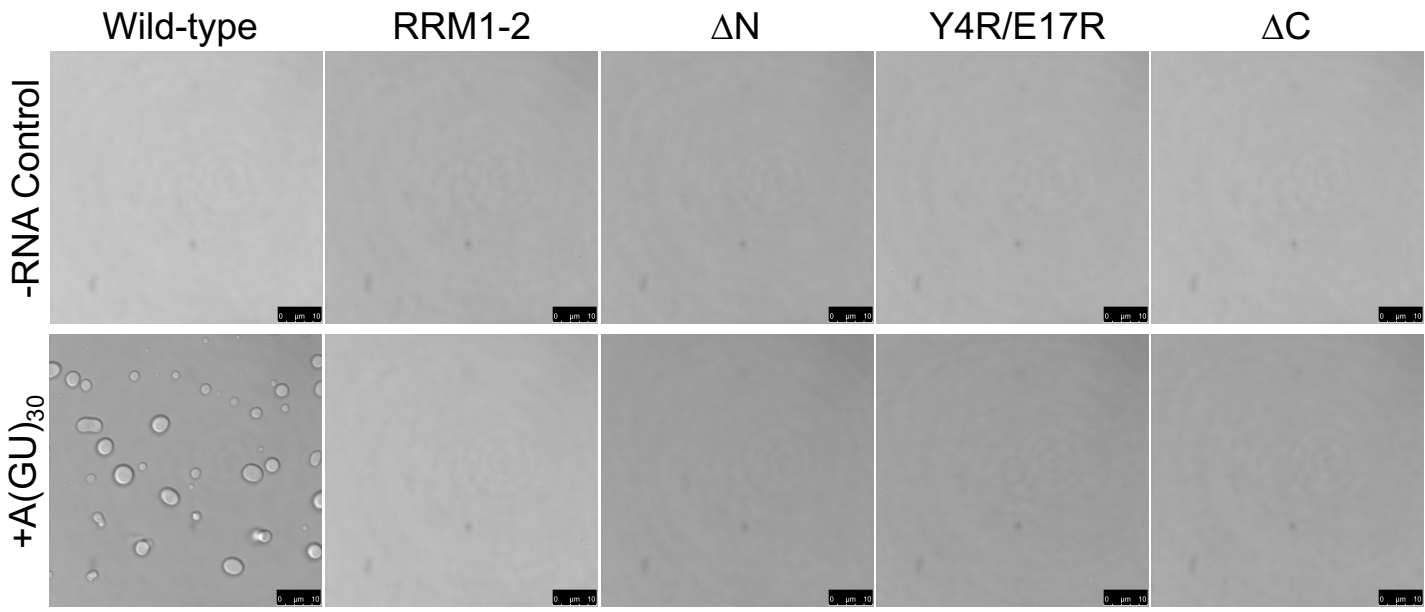

Wild-type
RRM1-2
ΔN
Y4R/E17R
ΔC
-RNA Control
+A(GU)30

Fig. 6

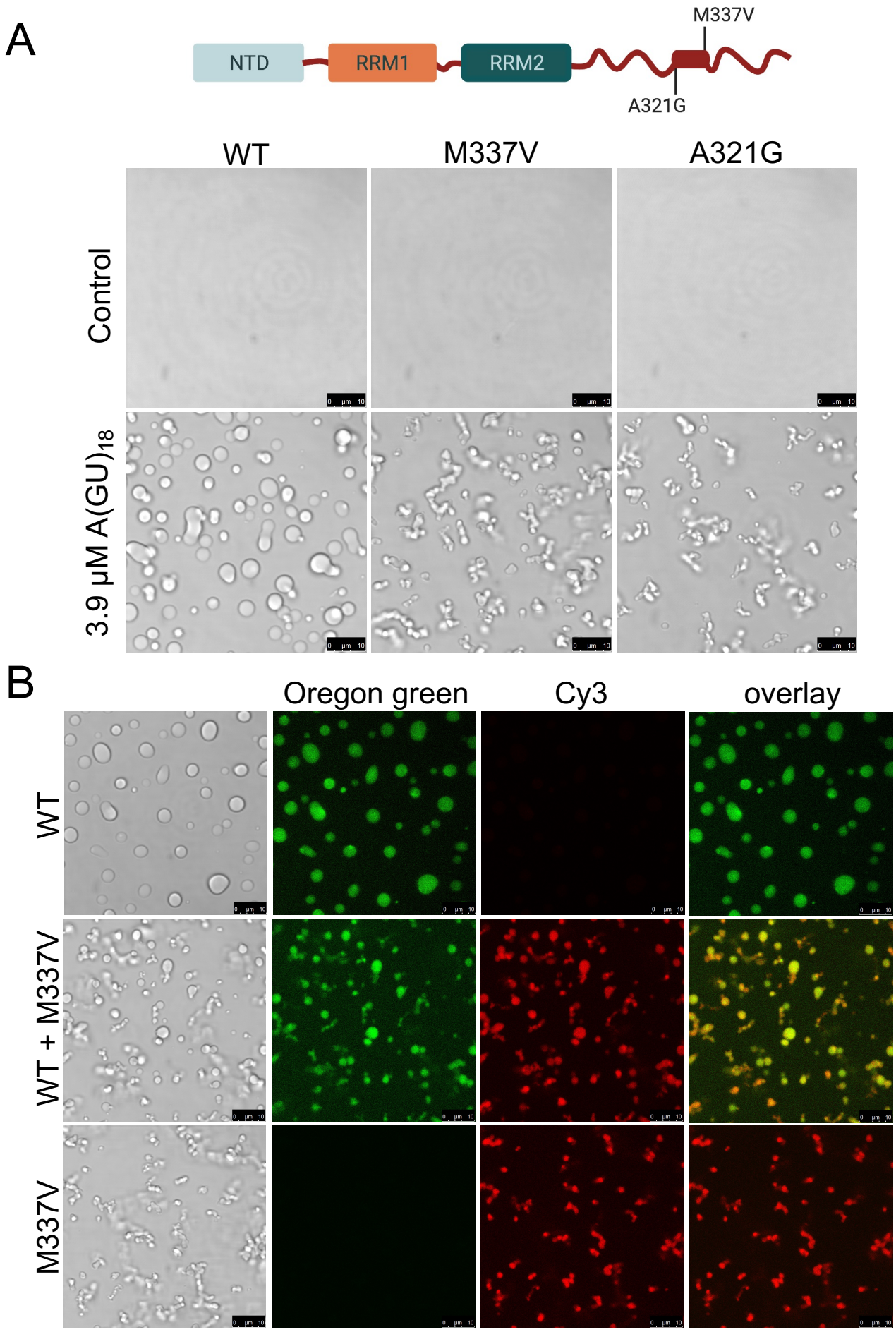
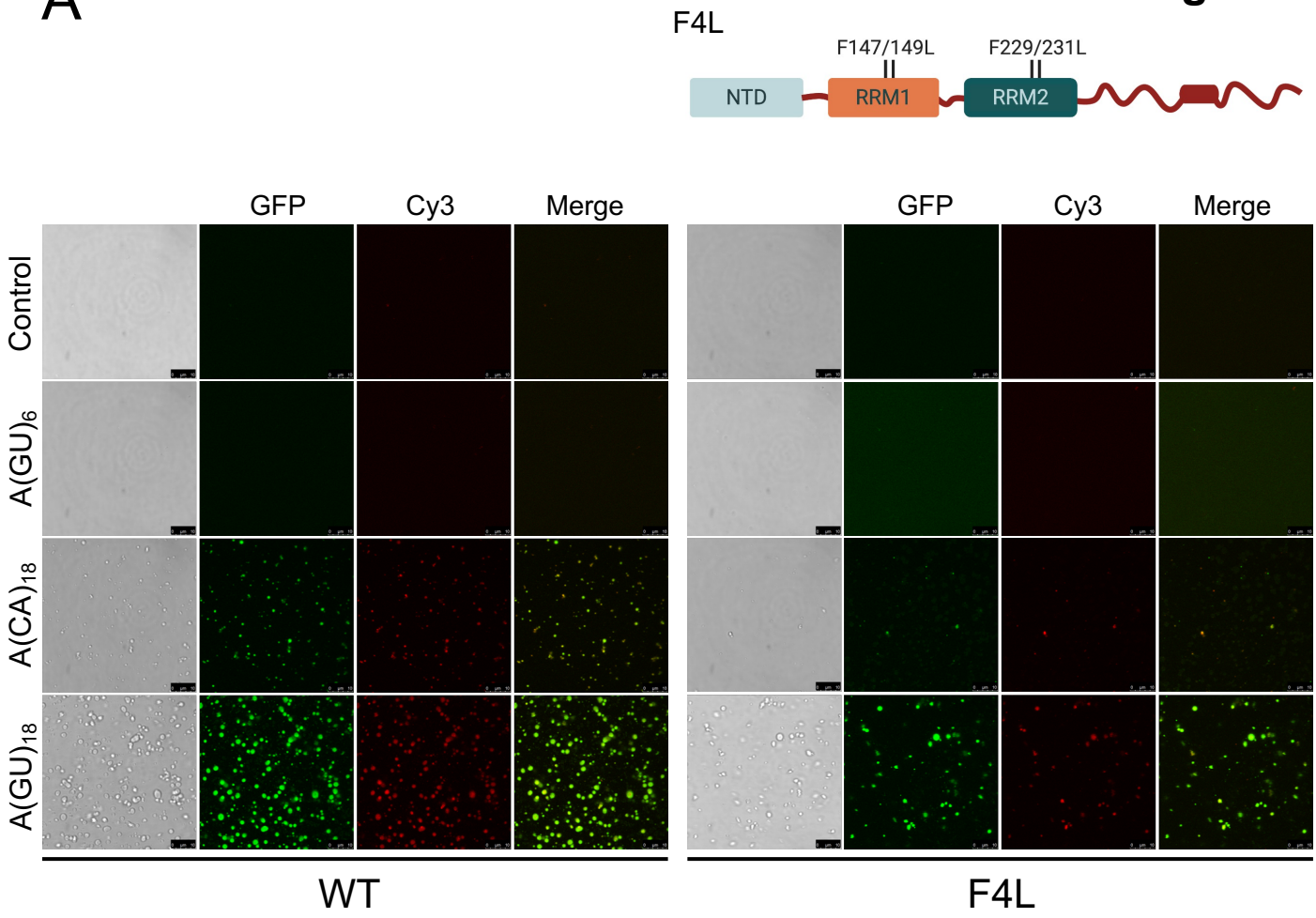

A
NTD
RRM1
RRM2
M337V
A321G
WT
M337V
A321G
Control
3.9 µM A(GU)18
B
Oregon green
Cy3
overlay
WT
WT + M337V
M337V

Fig. 7

A


F4L
F147/149L
F229/231L
NTD
RRM1
RRM2
GFP
Cy3
Merge
Control
A(GU)6
A(CA)18
A(GU)18
WT
F4L

B

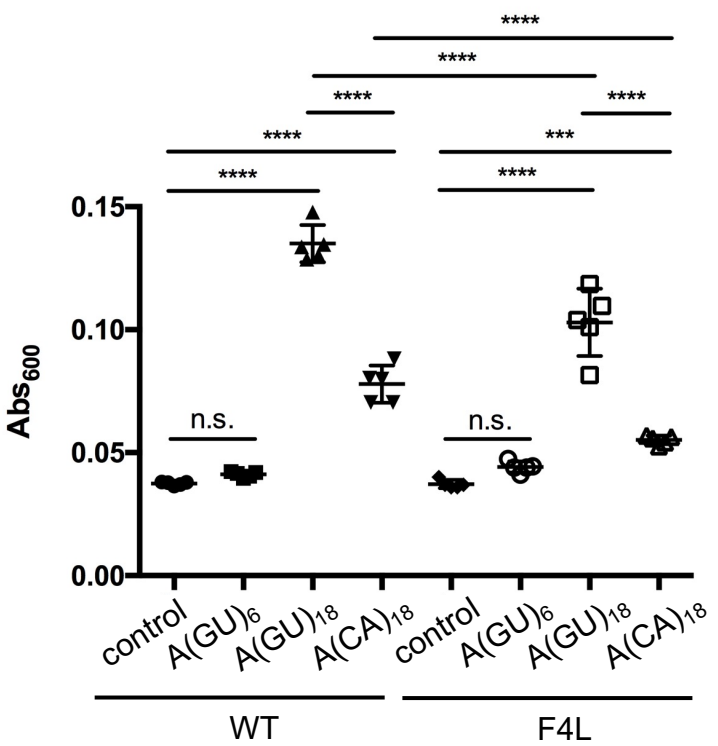
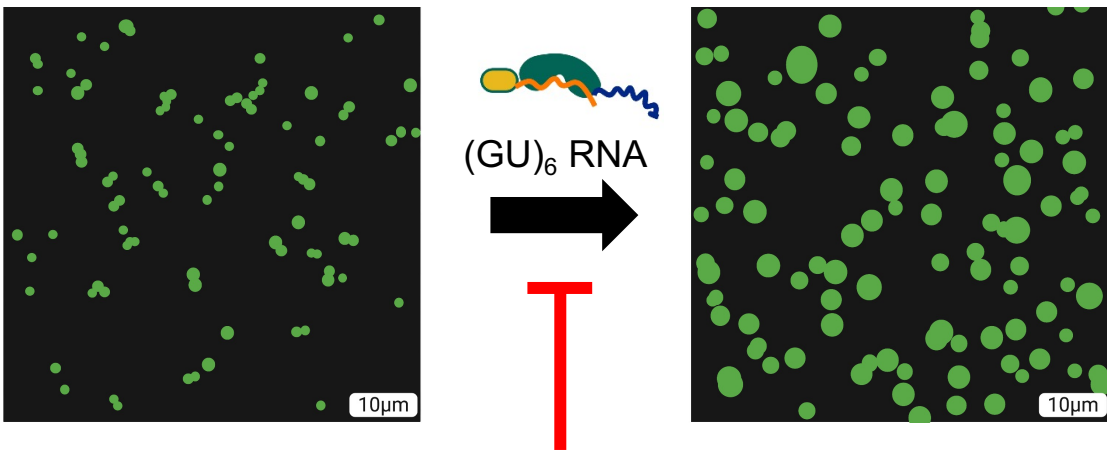

****
****
****
****
***
****
****
n.s.
n.s.
0.15
0.10
0.05
0.00
Abs600
control
A(GU)6
A(GU)18
A(CA)18
control
A(GU)6
A(GU)18
A(CA)18
WT
F4L

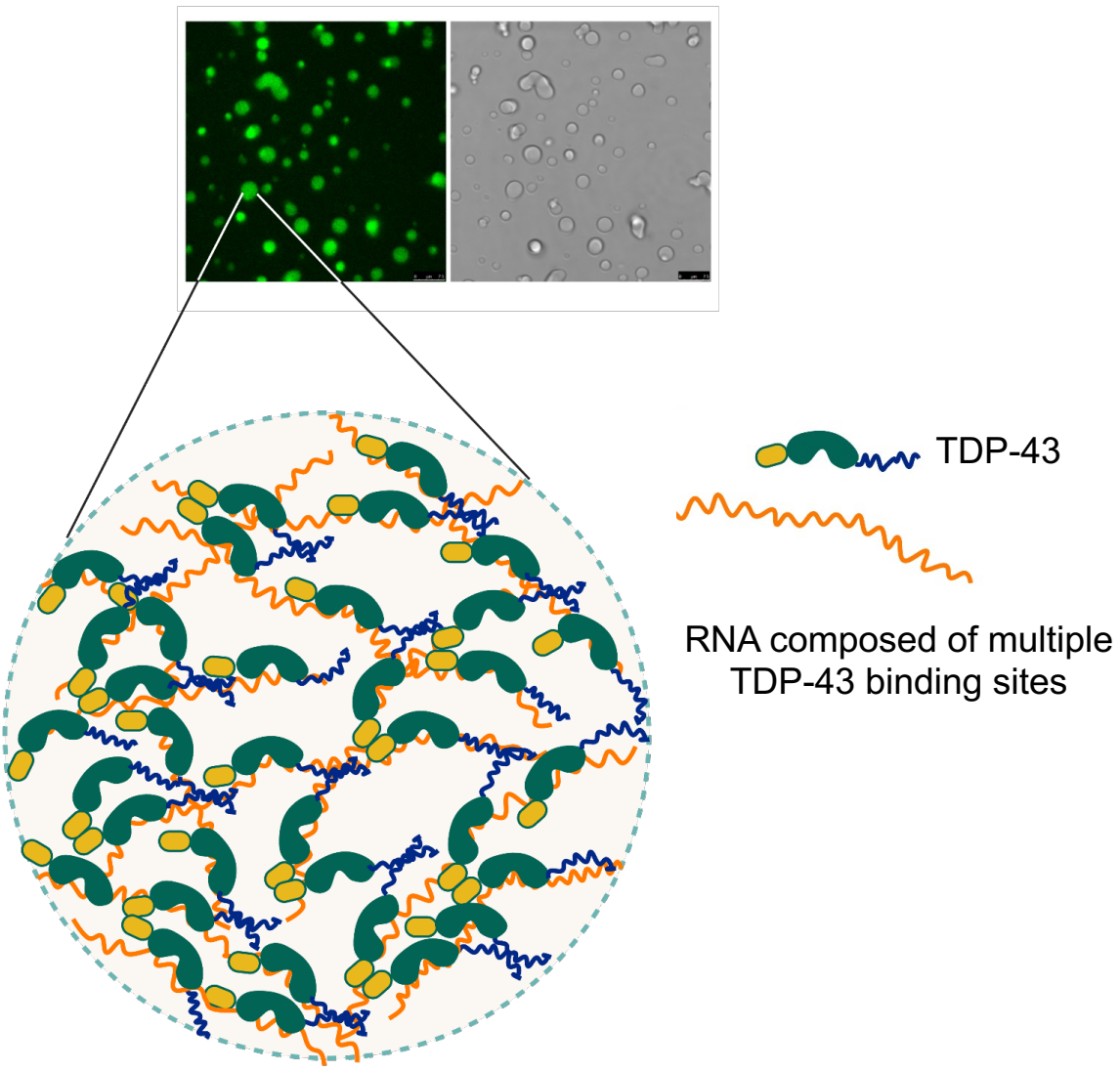
Fig. 8

A



Loss of specific RNA binding or ALS mutations

B



Supplementary Information

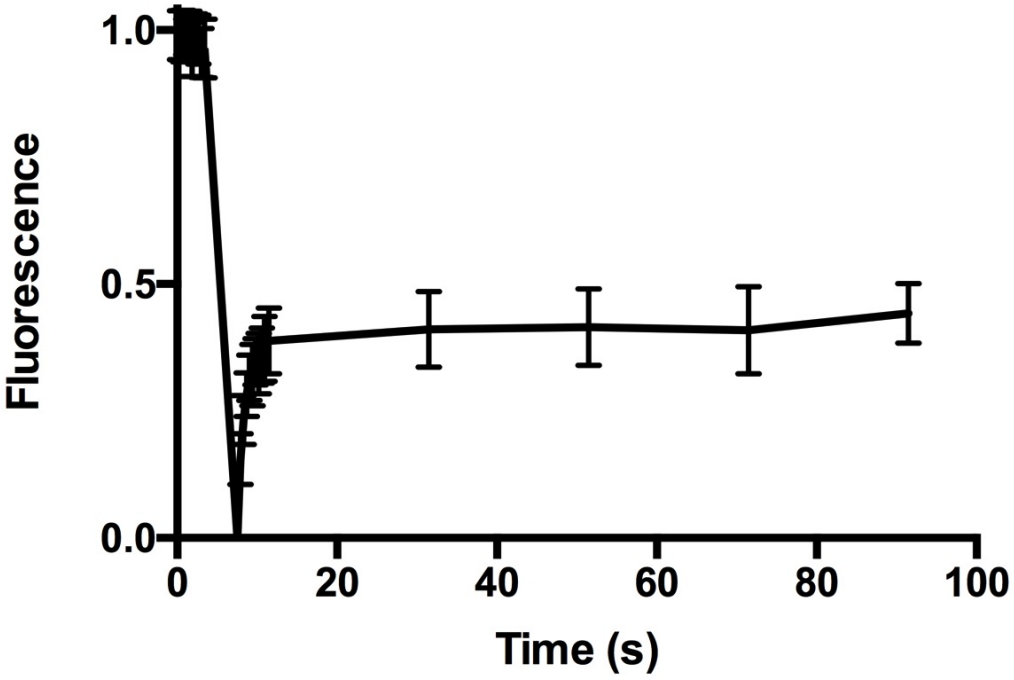
Specific RNA interactions promote TDP-43 multivalent phase separation and maintain liquid properties

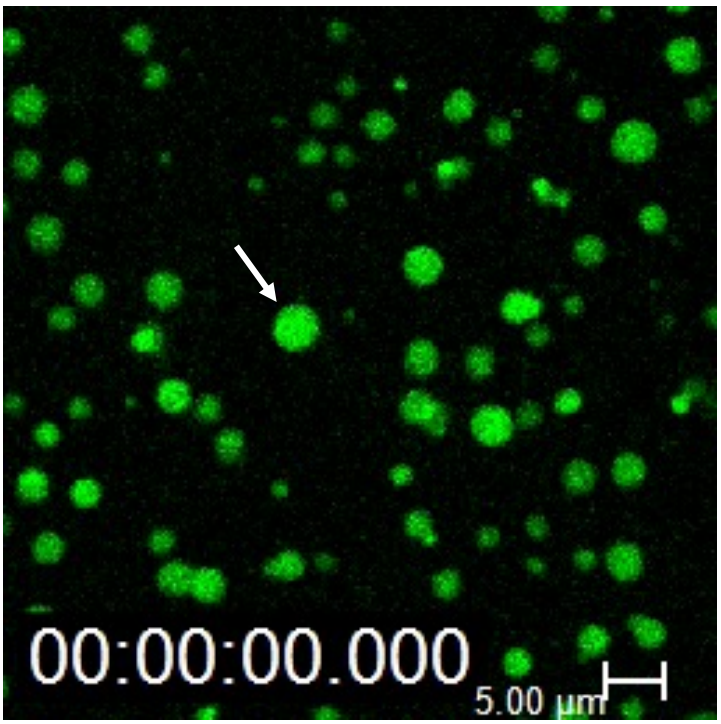
Zachary R. Grese[1], Alliny C.S. Bastos[1], Lohany D. Mamede[1], Rachel L. French[1], Timothy M. Miller[2] and Yuna M. Ayala[1*]

[1]Edward Doisy Department of Biochemistry and Molecular Biology, Saint Louis University, St. Louis, MO 63104.

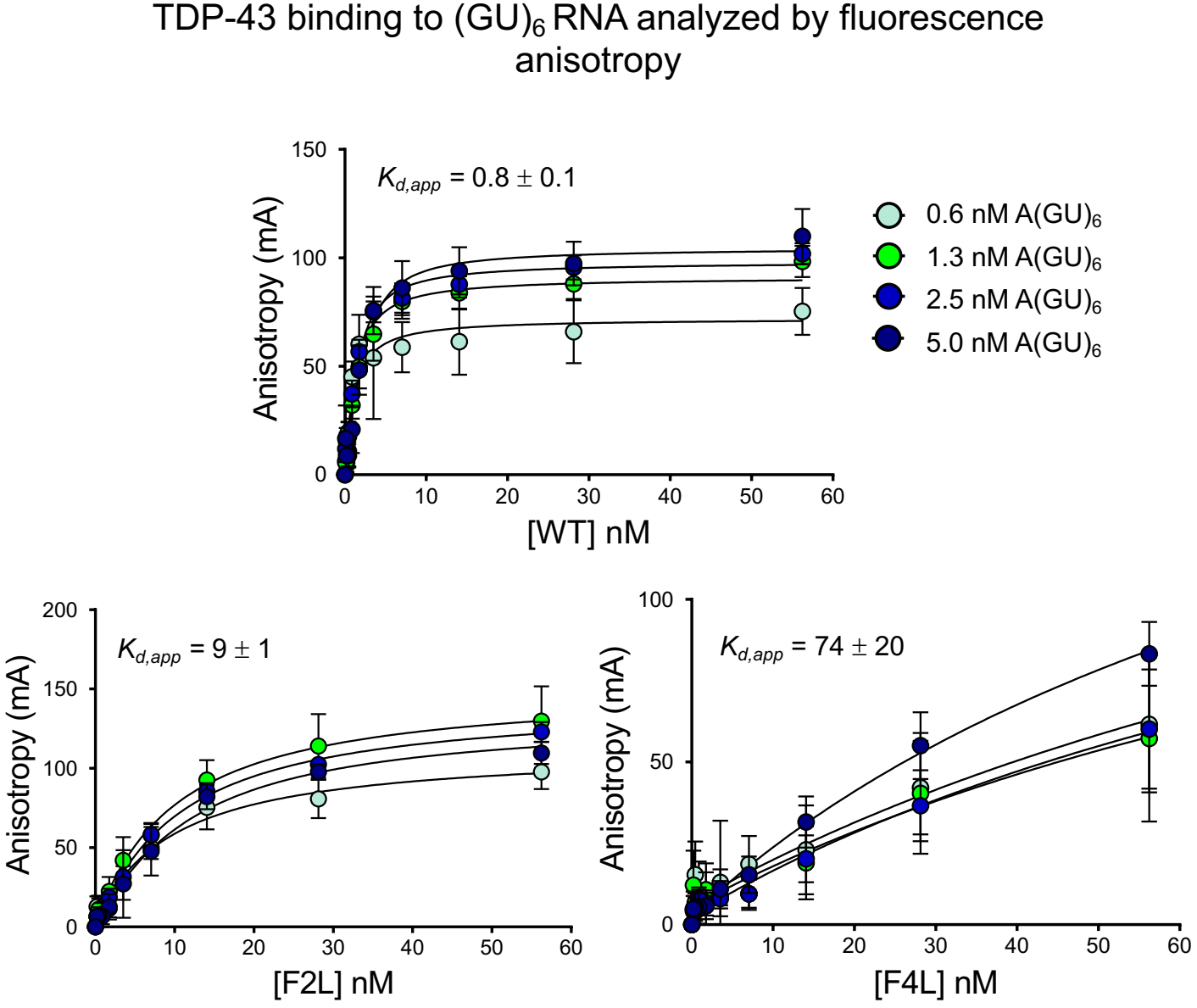
[2]Department of Neurology, Washington University School of Medicine, St. Louis, MO 63110.

*Corresponding author.

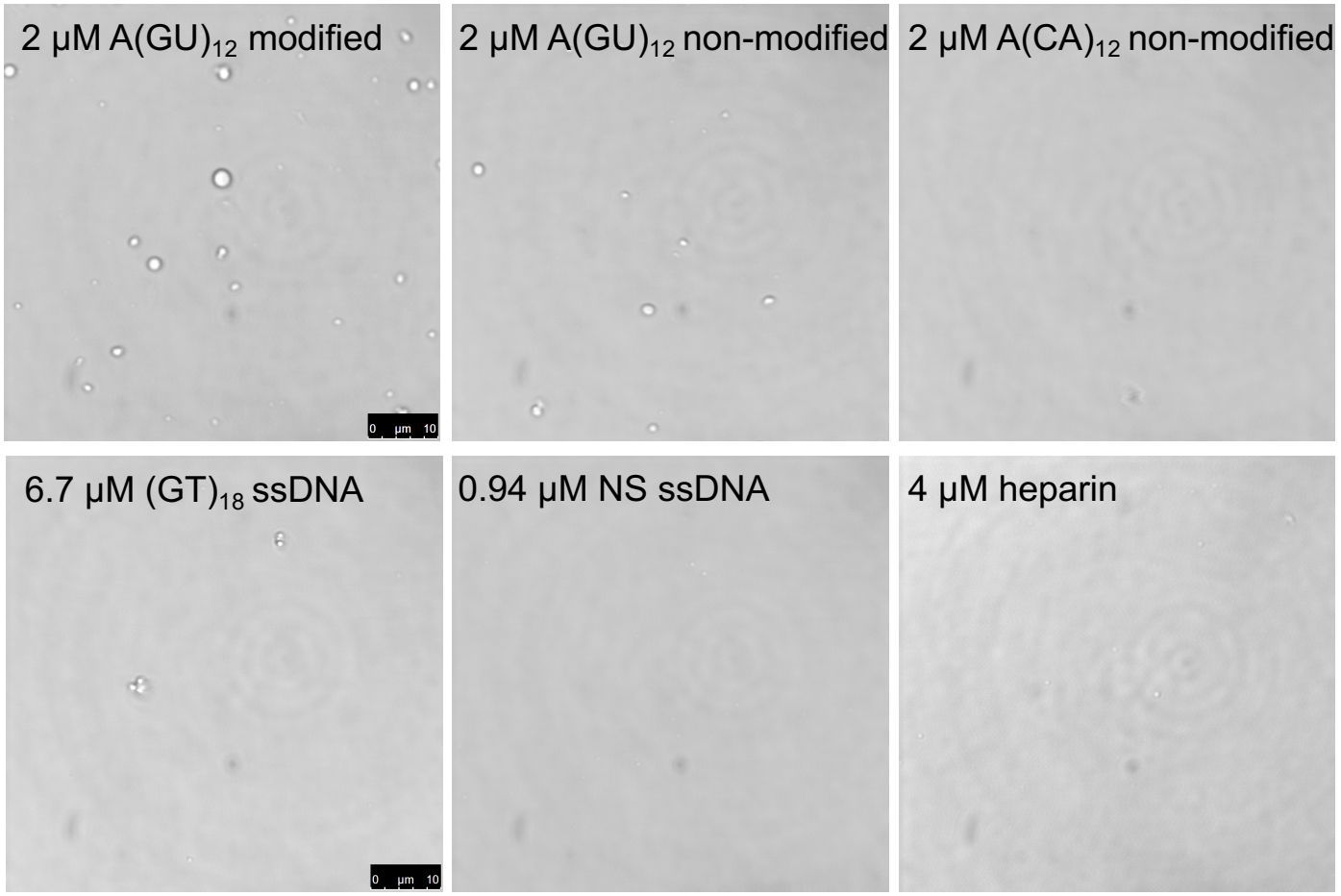




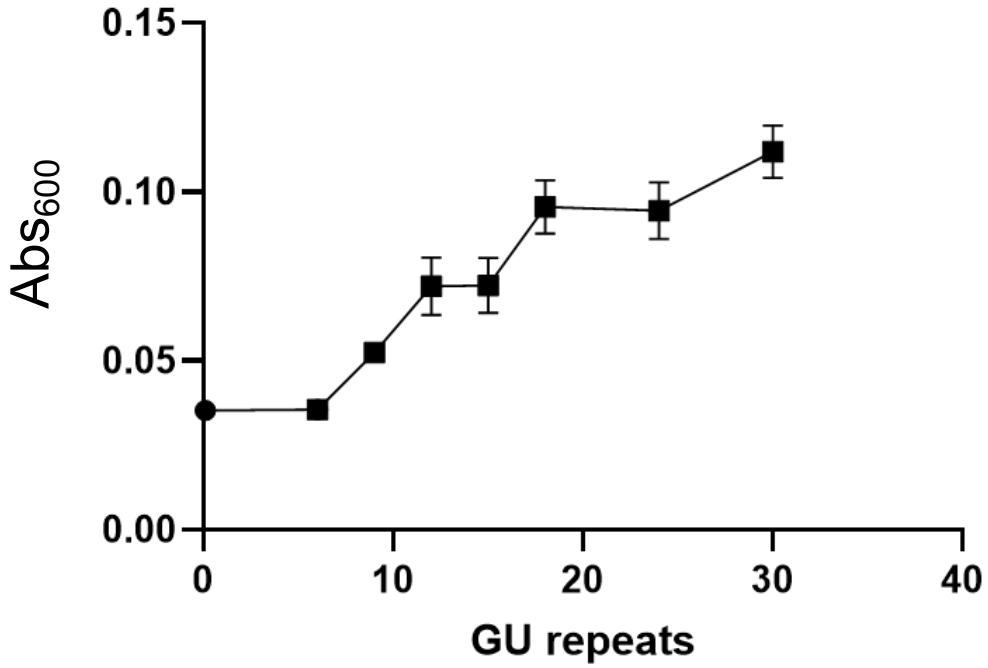
Supplementary Figure 1. TDP-43 RNA-driven LLPS of TDP-43 observed by fluorescence recovery after photobleaching (FRAP). Quantification of FRAP of TDP-43 droplets with $A(GU)_6$ RNA. 4 uM TDP-43 was mixed with 8 uM $A(GU)_6$ RNA at 150 mM NaCl. Mean values and SD from 3 independent experiments and 14 replicates, performed from 2 different protein purifications. Arrow points to a representative droplet bleached, scale bar 5 µm.



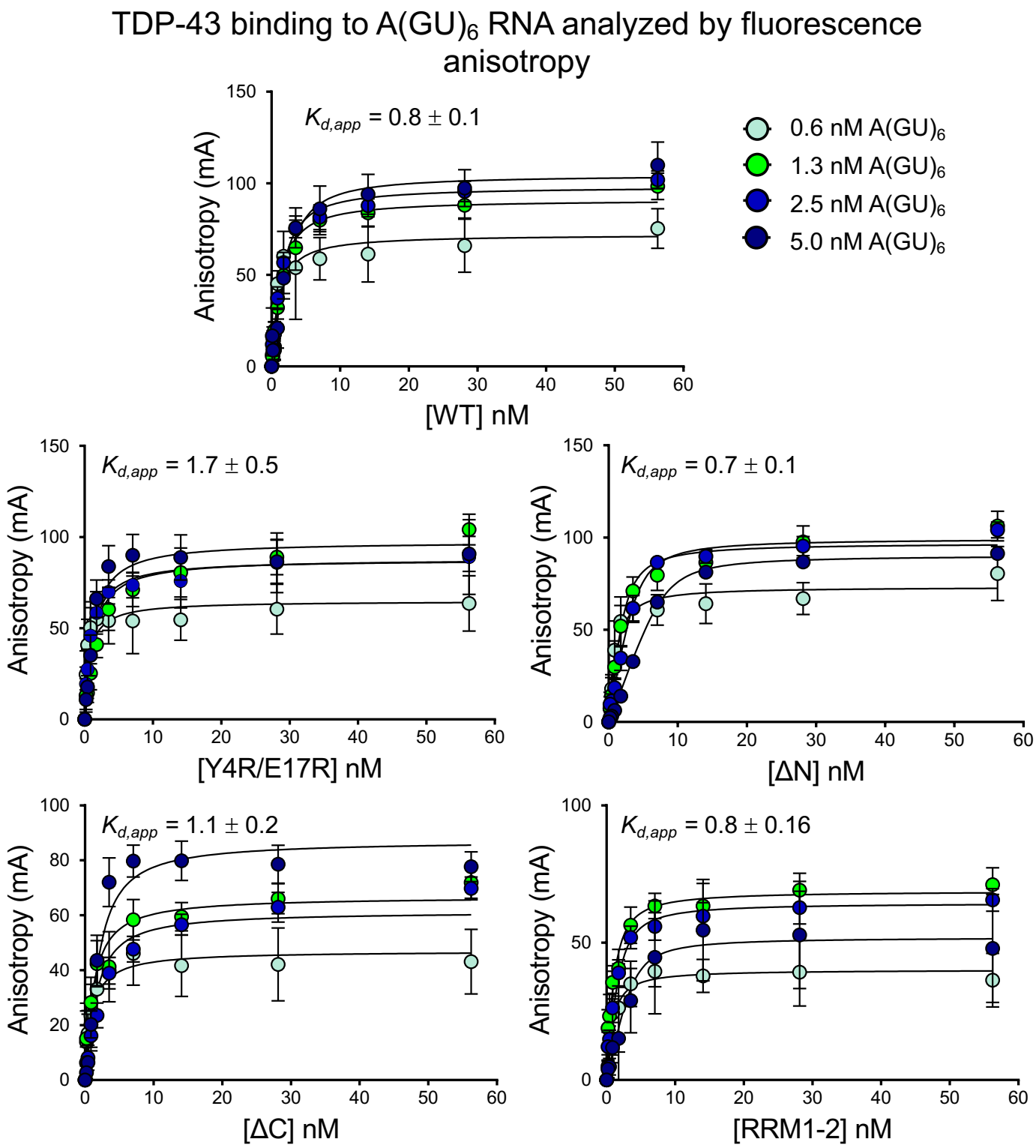
Supplementary Figure 2. TDP-43 binding to $(GU)_6$ RNA analyzed by fluorescence anisotropy. Fluorescence anisotropy of different FITC-labeled $A(GU)_6$ concentrations titrated with increasing TDP-43 WT and mutants (0-65 nM). Each point is the average of >3 replicates and 3 independent experiments (SEM). Solid lines represent the best global fit to calculate the apparent dissociation constant, $K_{d,app}$ (**Table 1**).



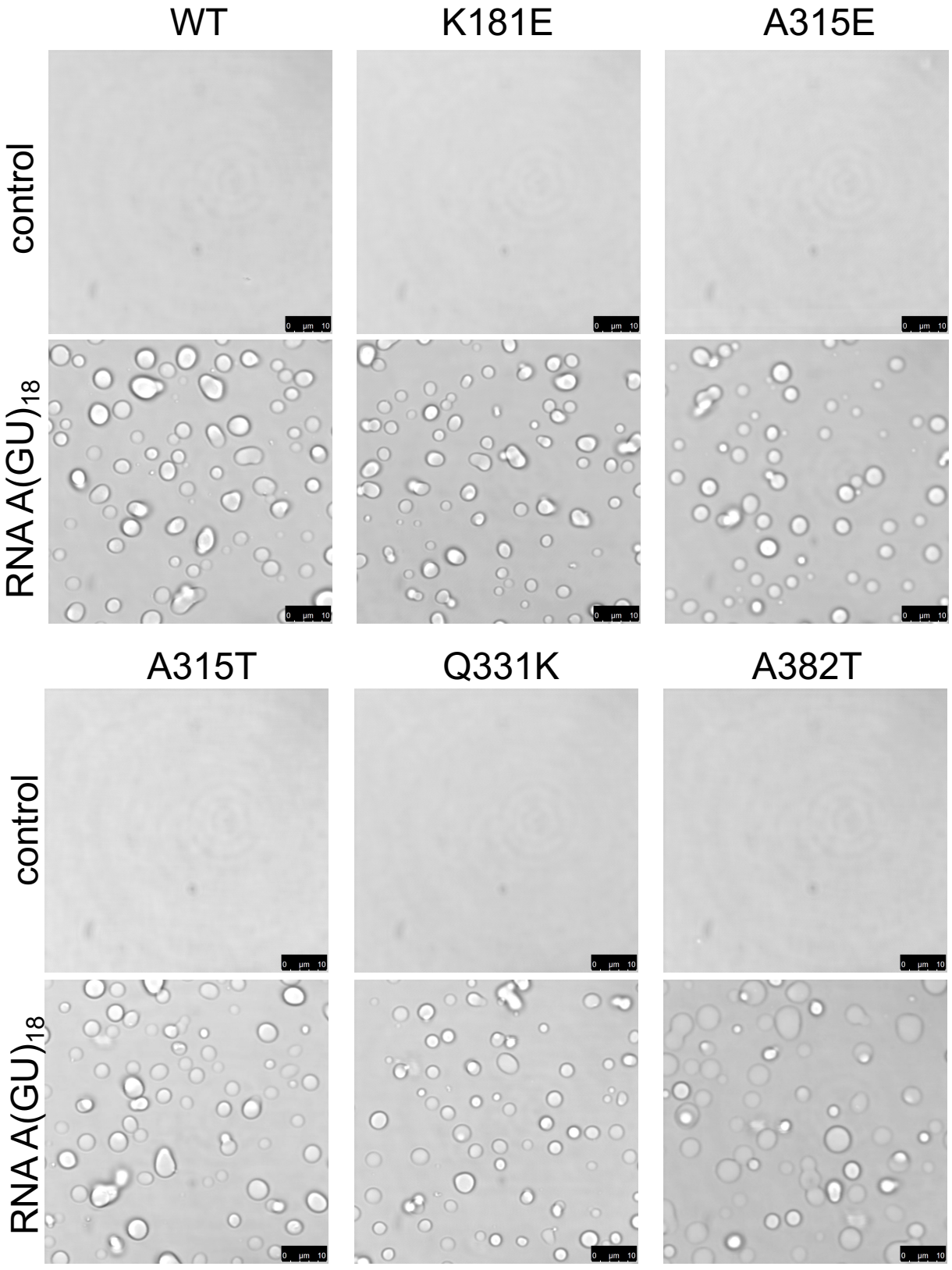
Supplementary Figure 3. RNA with multiple binding sites specifically triggers TDP-43 LLPS. TDP-43 LLPS observed by brightfield microscopy in the presence of $A(GU)_{12}$ and two sequences of non-modified RNA, $A(GU)_{12}$ and $(CA)_{12}$ at 250 mM NaCl . Lower panels show TDP-43 LLPS in the presence of single stranded DNA that binds TDP-43 with >100-fold lower affinity than GU-repeat RNA, $(GT)_{18}$, non-specific single stranded DNA NS (**Supplementary Table I**), and heparin. Representative images for 3 independent experiments with 2 different protein preparations.



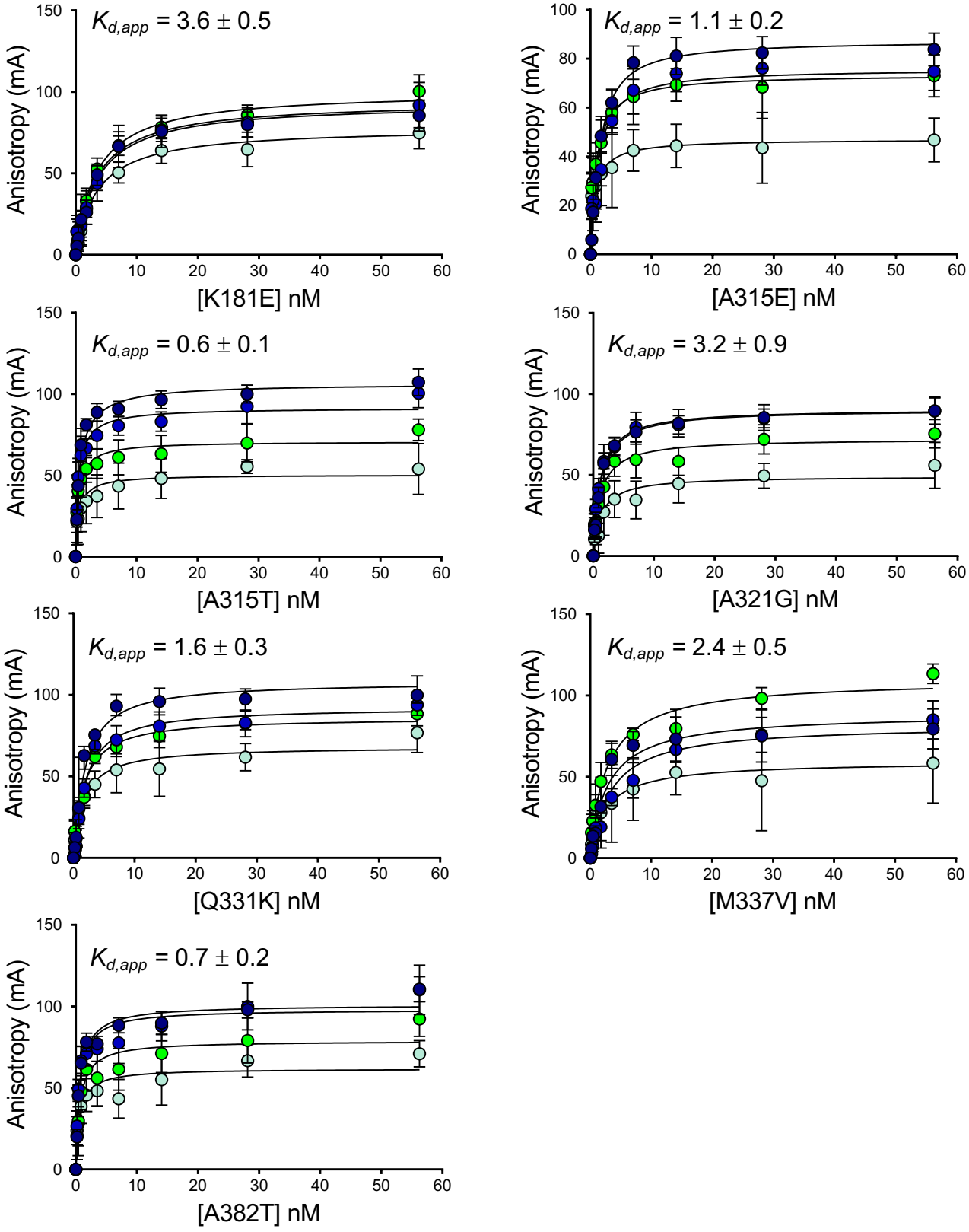
Supplementary Figure 4. GU-rich RNA promotes TDP-43 LLPS in a length dependent manner. Spontaneous TDP-43 phase separation in the presence of no RNA control and RNA oligonucleotides with increasing number of GU repeats at 250 mM NaCl. LLPS was measured by turbidity and plotted as a function of GU dinucleotide repeat number. RNA oligonucleotide concentration varied to maintain the concentration of putative binding sites constant. Mean values and SD from 3 independent experiments and 8 replicates, performed with 2 different protein preparations.



Supplementary Figure 5. TDP-43 binding to $(GU)_6$ RNA analyzed by fluorescence anisotropy. Fluorescence anisotropy of different FITC-labeled $A(GU)_6$ concentrations titrated with increasing TDP-43 WT and mutants (0-65 nM). Each point is the average of >3 replicates and 3 independent experiments (SEM). Solid lines represent the best global fit to calculate the apparent dissociation constant, $K_{d,app}$ (**Table 1**).



Supplementary Figure 6. LLPS of ALS-linked TDP-43 mutants induced by $(GU)_{18}$ RNA. Droplet formation of TDP-43 wild-type (WT) and ALS-associated mutations observed by brightfield microscopy in the presence of RNA, with $A(GU)_{18}$ (3.9 μM) and no RNA control at 250 mM NaCl. Representative images for 3 independent experiments with 3 and 2 different protein preparations of WT and K181E, respectively, and one preparation of A315E, A315T, Q331K and A382T. Scale bars, 10 μm.



Supplementary Figure 7. ALS-linked TDP-43 mutants binding to (GU)6 RNA analyzed by fluorescence anisotropy. Fluorescence anisotropy of different FITC-labeled $A(GU)_6$ concentrations titrated with increasing TDP-43 WT and M337V (0-65nM). Each point is the average of >3 replicates and 3 independent experiments (SEM). Solid lines represent the best global fit to calculate the apparent dissociation constant, $K_{d,app}$ (**Table 1**).

Supplementary Table 1. Oligonucleotide sequences used in phase separation assays

Name	RNA oligonucleotide sequence (5'-3')
$A(GU)_6$	AGUGUGUGUGUGU
$A(GU)_{18}$	AGUGUGUGUGUGUGUGUGUGUGUGUGUGUGUGUGU
CLIP34	GAGAGAGCGCGUGCAGAGACUUGGUGGUGCAUAA
$(AUG12)_3$	GUGUGAAUGAAUGUGUGAAUGAAUGUGUGAAUGAAU
$A(CA)_6$	ACACACACACACA
NS	CGCGACGGACGGAAAGACCCCUAUCCGUCGCG

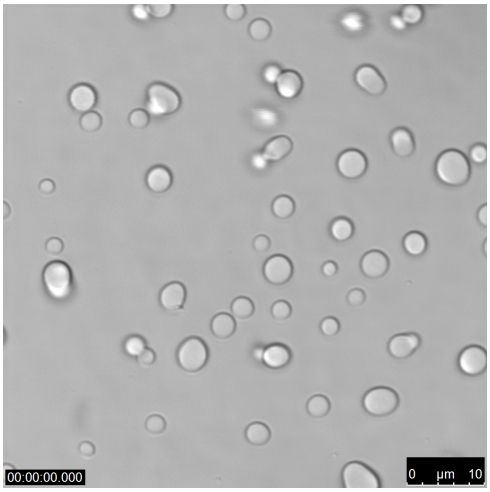
Name	DNA oligonucleotide sequence (5'-3')
$A(GT)_{18}$	AGTGTGTGTGTGTGTGTGTGTGTGTGTGTGTGTGT
NS ssDNA	CGCGACGGACGGAAAGACCCCUAUCCGUCGCG

Supplementary Table 2. DNA oligonucleotide sequences used for mutagenesis.

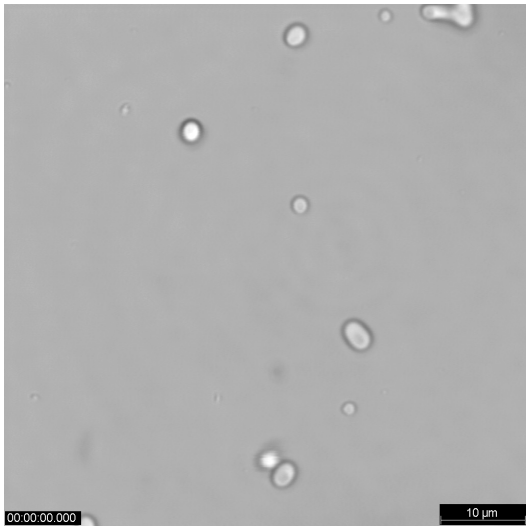
Name		RNA oligonucleotide sequence (5'-3')
Y4R/E17R		French RL, *et al.**
ΔN (102-414)		French RL, *et al.**
ΔC (1-269)		French RL, *et al.**
RRM1-2 (102-269)		French RL, *et al.**
F147/149L	FW	GACTGGTCATTCAAAGGGGCTTGGCCTTGTTCGTTTTACGGAATATG
	RV	CATATTCCGTAAAACGAACAAGGCCAAGCCCCTTTGAATGACCAGTC
F229/231L	FW	CCAAGCCATTCAGGGCCCTTGCCCTTGTTACATTTGCAGATGATC
	RV	GATCATCTGCAAATGTAACAAGGGCAAGGGCCCTGAATGGCTTGG
K181E	FW	GTGTGACTGCAAACTTCCTAATTCTGAGCAAAGCCAAGA
	RV	TCTTGGCTTTGCTCAGAATTAGGAAGTTTGCAGTCACAC
A315E	FW	GATGAACTTTGGTGAGTTCAGCATTAATC
	RV	GATTAATGCTGAACTCACCAAAGTTCATC
A315T		French RL, *et al.**
A321G	FW	TTTGGTGCTTCAGCATTAATCCAGGCATGATGGCTGCCGCCCAGGCAG
	RV	CTGCCTGGGCGGCAGCCATCATGCCTGGATTAATGCTGAACGCACCAAA
Q331K	FW	GCCGCCCAGGCAGCACTAAAGAGCAGTTGGGGTATGATG
	RV	CATCATACCCCAACTGCTCTTTAGTGCTGCCTGGGCGGC
M337V		French RL, *et al.**
A382T	FW	CTCTAATTCTGGTGCAACAATTGGTTGGGGATCAG
	RV	CTGATCCCCAACCAATTGTTGCACCAGAATTAGAG

Site mutations shown in red

*French RL, *et al.* Detection of TAR DNA-binding protein 43 (TDP-43) oligomers as initial intermediate species during aggregate formation. *J Biol Chem* **294**, 6696-6709 (2019).

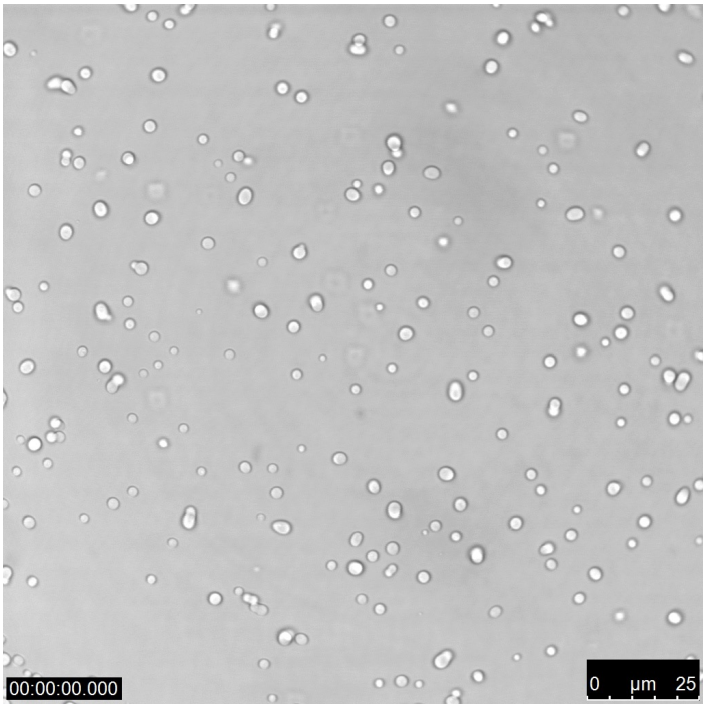


Supplementary Movie 1. TDP-43 droplets induced by RNA binding behave as liquid condensates. TDP-43 (4 µM) mixed with $A(GU)_{18}$ (6.5 µM) at 250 mM NaCl. Related to figure 1. Experiments were performed from 3 different protein preparations. Scale bars, 10 µm.



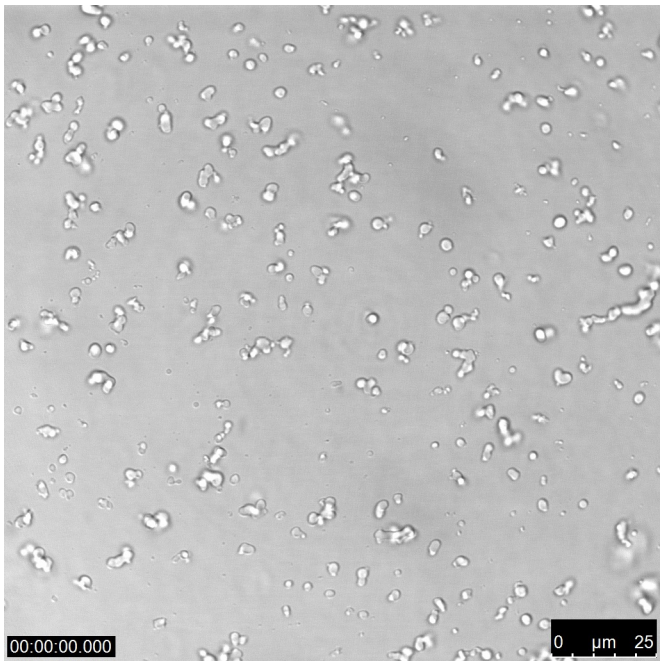
Supplementary Movie 2. TDP-43 droplets induced by RNA binding behave as liquid condensates. TDP-43 (4 µM) mixed with $A(GU)_{18}$ (1.3 µM) at 250 mM NaCl. Salt was added to the droplets at time 0 to increase the final salt concentration from 250 mM to 1.3 M. Related to figure 1. Experiments were performed from 2 different protein preparations. Scale bars, 10 µm.

Wild-type TDP-43 plus RNA



Supplementary Movie 3. ALS-linked TDP-43 mutation impairs the liquid-like behavior imparted by RNA binding. Movie following droplets formed by wild-type TDP-43 (4 µM) after mixing with $A(GU)_{18}$ (6.5 µM) at 250 mM NaCl. Related to figure 6. Experiments were performed from 3 different protein preparations. Scale bars, 25 µm.

M337V plus RNA



Supplementary Movie 4. ALS-linked TDP-43 mutation impairs the liquid-like behavior imparted by RNA binding. Movies following droplets formed by the ALS-linked mutant M337V TDP-43 (4 µM) after mixing with $A(GU)_{18}$ (6.5 µM) at 250 mM NaCl. Related to figure 6. Experiments were performed from 3 different protein preparations. Scale bars, 25 µm.